



PCCP

**Generalised Dissipative Particle Dynamics with Energy Conservation: Density and Temperature-Dependent Potentials**

Journal:	<i>Physical Chemistry Chemical Physics</i>
Manuscript ID	CP-ART-08-2019-004404.R1
Article Type:	Paper
Date Submitted by the Author:	10-Oct-2019
Complete List of Authors:	Bonet Avalos, Josep; Universitat Rovira i Virgili, ETSEQ, Enginyeria Química Lisal, Martin; ICPF, Larentzos, James; US Army Research Laboratory, Weapons and Materials Research Directorate Mackie, Allan; Universitat Rovira i Virgili, Brennan, John; U.S. Army Research Laboratory, Weapons and Materials Research Directorate

SCHOLARONE™  
Manuscripts

Cite this: DOI: 00.0000/xxxxxxxxxx

# Generalised Dissipative Particle Dynamics with Energy Conservation: Density- and Temperature-Dependent Potentials †

Josep Bonet Avalos,<sup>a</sup> Martin Lísal,<sup>b,c</sup> James P. Larentzos,<sup>d</sup> Allan D. Mackie,<sup>a</sup> and John K. Brennan<sup>\*d</sup>

Received Date

Accepted Date

DOI: 00.0000/xxxxxxxxxx

We present a generalised, energy-conserving dissipative particle dynamics (DPDE) method appropriate for the non-isothermal simulation of particle interaction force fields that are both density- and temperature-dependent. A detailed derivation is formulated in a bottom-up manner by considering the thermodynamics of small systems with the appropriate consideration of the fluctuations. Connected to the local volume is a local density and corresponding local pressure, which is determined from an equation-of-state based force field, depending also on a particle temperature. Compared to the original DPDE method, the formulation of the generalised DPDE method requires a change in the independent variable from the particle internal energy to the particle entropy. As part of the re-formulation, the terms dressed particle entropy and the corresponding dressed particle temperature are introduced, which depict the many-body contributions in the local volume. The generalised DPDE method has similarities to the energy form of the smoothed dissipative particle dynamics method, yet fundamental differences exist, which are described in the manuscript. The basic dynamic equations are presented along with practical considerations for implementing the generalised DPDE method, including a numerical integration scheme based on the Shardlow-like splitting algorithm. Demonstrations and validation tests were performed using analytical equation-of-states for the van der Waals and Lennard-Jones fluids. Particle probability distributions were analysed, where excellent agreement with theoretical estimates was demonstrated. As further validation of the generalised DPDE method, both equilibrium and non-equilibrium simulation scenarios were considered, including adiabatic flash heating response and vapour-liquid phase separation.

## 1 Introduction

Heat transport in nanometric dimensions is a generic problem found in many disciplines and situations, ranging from molecular motors, chemical reactions in nanocapsules<sup>1</sup>, microelectronic systems<sup>2,3</sup>, propagation of reactive fronts<sup>4,5</sup>, and nanolubrication<sup>6</sup>, among others<sup>7,8</sup>. In many of these cases, the temperature gradients may lay in the range  $10^6 - 10^8$  K/m. In these very large

temperature gradients, the coupling between the different non-equilibrium processes is critical for both the understanding as well as modelling of energy transfer phenomena at the nanoscale. In other situations, there is evidence of interfacial heat conductivity depending on the surface roughness<sup>9</sup>, polarisation of water molecules due to temperature gradients<sup>10,11</sup>, and heat rectification at the nanoscale<sup>12,13</sup>. Molecular dynamics simulations have been applied to the calculation of interfacial heat transfer coefficients<sup>14,15</sup>. However, the analysis of significantly larger systems, still under the submicrometric scale, cannot be addressed by the direct application of molecular dynamics simulations because the computational cost would be prohibitive.

Coarse-grain (CG) modelling and simulation offers an alternative route for such cases when molecular simulations are too computationally expensive. The simplest CG models, used for example in the original formulations of the DPDE algorithms, are separation-distance dependent models; however, the more accurate models for specific quantitative applications typically con-

<sup>a</sup> Department d'Enginyeria Química, ETSEQ, Universitat Rovira i Virgili, Tarragona, Spain.

<sup>b</sup> Department of Molecular and Mesoscopic Modelling, Institute of Chemical Process Fundamentals of the CAS, Prague, Czech Republic.

<sup>c</sup> Department of Physics, Faculty of Science, J. E. Purkinje University, Ústí n. Lab., Czech Republic.

<sup>d</sup> Weapons and Materials Research Directorate, U.S. Army Combat Capabilities Development Command Army Research Laboratory, Aberdeen Proving Ground, MD, USA.

\* E-mail: john.k.brennan.civ@mail.mil; Fax: 410 306 1909; Tel: 410 306 0678

† Electronic Supplementary Information (ESI) available: The ESI contains additional modelling details and results. See DOI: 00.0000/00000000.

tain a density dependence that accounts for many-body interactions, which are the result of the coarsening of the degrees-of-freedom from the coarse-graining process. The density dependence improves transferability of the model accuracy outside of the parameterisation limits. Moreover, in some cases, CG models that are both density- and temperature-dependent have been shown necessary for further improvement of both the accuracy and transferability. Indeed, a growing trend towards density- and temperature-dependent CG models is slowly emerging. Such models may be built from higher resolution models (e.g., ref. 16), or may be a many-body force field based on an analytical equation-of-state (MB-FF-EOS) (e.g., ref. 17). To date, these density- and temperature-dependent CG models typically have been simulated at isothermal conditions. In other non-isothermal cases, the temperature enters into the definition of the model parametrically, not as the intrinsically fluctuating particle temperature<sup>18,19</sup>.

In the context of implementing CG models into an appropriate non-isothermal CG methodology, Dissipative Particle Dynamics with energy conservation (DPDE)<sup>20,21</sup> is a CG method that has proven its applicability in a wide range of situations<sup>22–27</sup>, including shock wave propagation<sup>4,5,28–31</sup>, and other applications<sup>32,33</sup>. However, additional considerations arise when implementing a density- and temperature-dependent force field within the DPDE framework, since both the local density and particle temperature are fluctuating and contribute to the forces between particles and interaction energies. In this work, we formulate the theory of DPDE for not only density-dependent<sup>17,31,34–36</sup> (see also<sup>27</sup> for a review), but also for temperature-dependent particle-particle interactions, suitable to cover the gap between atomistic molecular dynamics and the scale-invariant Smoothed Particle Hydrodynamics (SPH) method.

In contrast with SPH<sup>37,38</sup> and its fluctuating counterpart, Smoothed Dissipative Particle Dynamics (SDPD)<sup>39,40</sup>, DPDE is a bottom-up method, suitable for CG models that have been built using coarse-graining procedures that utilised high resolution models, and thus retains microscopic information about the underlying system. The parameters in SPH and SDPD are obtained from the macroscopic properties of the system after a discretisation of the macroscopic continuum fields using a smoothing kernel  $W$  with a characteristic range  $h$ , typically larger than, but of the order of the interparticle distance. The macroscopic fields then enter into the definition of the model linked to the characteristic chosen scale related to the virtual volume  $\mathcal{V}$  of the particle<sup>41</sup>. The variance of the fluctuations,  $\langle v^2 \rangle$ , is thus found to decrease as the size of the particle increases according to

$$\langle v^2 \rangle \sim D \frac{k_B T}{\rho \mathcal{V}} \quad (1)$$

where  $D$  is the dimensionality of the space,  $k_B$  is the Boltzmann constant,  $T$  is the temperature, and  $\rho$  is the characteristic mass density of the system. However, the systematic dynamics (with fluctuations set off, say) is scale invariant for wavelengths  $\lambda_0 > 1/\mathcal{V}^{1/D}$  as it reproduces the Navier-Stokes fluid dynamics. The transport coefficients of the model are further invariant provided that the additional condition  $\mathcal{V}^{1/D} \ll h$  is also satisfied, to

enforce that the pair distribution function  $g(|\mathbf{r} - \mathbf{r}'|) \simeq 1$  at all distances<sup>42–44</sup>. Therefore, introducing the adequate scaling of the fluctuations in eq. (1), SDPD can describe the behaviour of a suspended colloid of size  $R$  with any discretisation of the fluid  $\mathcal{V}$ , provided  $R \gg \lambda_0$ . This condition demands that there exists a large separation in scales between the dynamics of the suspended particle and the dynamics of the particles forming the CG fluid. This situation is common in many applications such as in suspensions, notably in all these situations that can be described within the framework of the Langevin equation<sup>45,46</sup>.

The cut-off length  $\lambda_0$  is however critical since as the size of the fluid particle decreases, the effect of the fluctuations increases. Therefore for small scales, the importance of the fluctuations is comparable to the importance of the conservative forces, thus breaking the scale invariance of SPH and SDPD methods, as well as the scaling of the fluctuations expressed in eq. (1). This disruption of the scale invariance for  $\lambda_0 \rightarrow 0$ , together with the definition of the fields from the macroscopic perspective, characterises SPH and SDPD as *top-down* methods.

As part of the discussion of the generalised DPDE method that is proposed here, we review the formulation of the thermodynamic description at the mesoscopic level, which includes a discussion of the role of the dependent and independent variables for systems with large fluctuations<sup>47,48</sup>. In this paper, we introduce an energetic formulation of a generalised DPDE method that requires a swap in independent variables. The need for an energetic formulation arises, in part, from the requirement of an integration algorithm based on the splitting of the conservative motions of the particles, here depending on particle temperatures, from heat exchange between them. Such a scheme thus requires adiabatic transformations in the system when the former are applied, which naturally suggests that the entropy of the particle, instead of the energy, should be the independent variable. However, since the entropy is inherently a non-conserved quantity, it is not suitable as the independent variable when the heat exchange step is considered.

The proposed algorithm introduces the aforementioned splitting of the conservative and dissipative interactions, together with the use of the particle internal energy as the independent variable, in a consistent manner. Moreover, we take advantage of this situation to introduce an illustrative analysis of the consistency of the model, and its thermodynamic properties in the canonical ensemble, in contrast with the usual formulation in the microcanonical ensemble<sup>27</sup>, although both analyses are equivalent. The advantage of the canonical ensemble is that the system temperature is externally characterised, and not defined in terms of the energy of the system, as it occurs within the microcanonical ensemble, making the derivation more transparent. The algorithm is independent of the reservoir temperature and is suitable for the simulation of thermally isolated systems as well. This study is carried out in Sec. 2, where a detailed derivation is presented that is formulated in a bottom-up manner by considering the thermodynamics of small systems, ensuring a link to the underlying physical system of the higher resolution model.

In Sec. 3, we provide detailed derivations of the dynamic equations, first for the reversible (conservative) interactions based

on the mesoscopic thermodynamic description, and then for the irreversible (dissipative) interactions. The equations-of-motion (EOM) and fluctuation-dissipation relations for the generalised DPDE method are given in Sec. 4, which includes practical considerations regarding the numerical integration of the algorithm under the form of a Shardlow-like splitting algorithm<sup>26,49</sup>. Applications and demonstrations of the generalised DPDE method for the van der Waals and Lennard-Jones fluids at both equilibrium and non-equilibrium conditions are considered in Sec. 5.

## 2 Mesoscopic thermodynamics considerations

### 2.1 Definition of the internal state of the DPDE particle

Let us consider that the DPDE particle in our generalised method is a material element embodying many physical constituents. This vision has been discussed in several references, notably through the tessellation of a physical system first introduced by Flekkøy and coworkers<sup>50,51</sup>. Let us assume that each CG particle contains some number of coarsened degrees-of-freedom. Here, for the sake of simplicity, we will ignore the dependence of the parameters on the latter, but whose effect will be studied elsewhere. Throughout this work, we use the following terminology: *macroscopic* refers to the thermodynamic system, *mesoscopic* refers to the DPDE or CG system, while *microscopic* refers to the underlying physical system that is represented by the DPDE particle.

Let us consider an ensemble of  $N$  DPDE particles ( $i = 1, \dots, N$ ) located at the space points  $\{\mathbf{r}_i\}_{i=1}^N$ . A local density of DPDE particles is estimated from the expression<sup>34,36</sup>

$$n_i \equiv \frac{\sum_{j \neq i} w(r_{ij})}{[w]} \quad (2)$$

with  $r_{ij} = |\mathbf{r}_{ij}|$ ,  $\mathbf{r}_{ij} = \mathbf{r}_i - \mathbf{r}_j$  and

$$[w] \equiv \int w(r) d\mathbf{r} \quad (3)$$

$w(r)$  is a smooth, non-negative, spherically symmetric weighting function vanishing for  $r \geq R_{cut}$ , where  $R_{cut}$  is the cut-off range. Specific forms of  $w(r)$  are discussed below. Notably,  $n_i$  provides a measure of the *volume* of the DPDE particle,  $\mathcal{V}_i \equiv 1/n_i$ . Such particle volumes are not additive since  $V \neq \sum_i \mathcal{V}_i$ , where  $V$  is the volume of the system. However, under normal conditions (e.g., homogeneous fluids) these two magnitudes should not significantly differ. Furthermore, with the definition of eq. (2)<sup>36</sup>, an isolated particle can have an undefined value of the local density because  $n_i < 1/R_{cut}^3$ , but the integration of eq. (3) returns  $n_i = 0$ , if a cut-off is used. This is an artifact of the cut-off, which has to be addressed in the simulations of the model we present. Alternatively, the local density can be defined using the Voronoi tessellation<sup>52</sup>, which leads to  $V = \sum_i \mathcal{V}_i$ .

For the internal state of the DPDE particle, we will assume there exists a function  $u_i$  of the collective properties of the internal coarsened degrees-of-freedom. The function  $u_i$  is considered to depend upon the mesoscopic equivalent of the macroscopic ther-

modynamic variables that define the state of a given system, i.e.

$$u_i = u_i(s_i, n_i) \quad (4)$$

where  $s_i$  is a measure of the mesoscopic *bare particle entropy* of the DPDE particle<sup>53</sup>. We assume that the state of this particle is only changed through the exchange of heat with neighbouring particles, and through changes in the local volume via the variation of its arguments  $s_i$  and  $n_i$ . Depending on the nature of the underlying microscopic physical system, other variables may be considered. Furthermore, we can define intensive-like variables from the expression

$$du_i = \theta_i ds_i + \frac{\pi_i}{n_i^2} dn_i \quad (5)$$

where the particle temperature is defined as

$$\theta_i \equiv \left. \frac{\partial u_i}{\partial s_i} \right|_{n_i} > 0 \quad (6)$$

$\theta_i$  must be strictly positive, so that the inverse function  $s_i = s_i(u_i, n_i)$  exists<sup>54</sup>. By analogy, we have introduced the particle pressure according to

$$\pi_i \equiv n_i^2 \left. \frac{\partial u_i}{\partial n_i} \right|_{s_i} \quad (7)$$

We will assume that the first law of thermodynamics, which includes irreversible processes, holds also at the mesoscopic (particle) level, namely

$$du_i = dq_i + dW_i \quad (8)$$

where  $dq_i$  and  $dW_i$  are, respectively, the total heat transferred by the particle  $i$  and the work done onto it. According to eqs. (5) and (8), we can write

$$\begin{aligned} \theta_i ds_i &= dq_i + dW_i - \frac{\pi_i}{n_i^2} dn_i \\ &= dq_i + dW_i^{irrev} \end{aligned} \quad (9)$$

where in the last term we have introduced the irreversible work exerted on the particle.

### 2.2 Equilibrium averages and appropriate estimators

In the context of the generalised DPDE method, let us consider the canonical ensemble, defined by a temperature  $T$ , a volume  $V$  and number of DPDE particles  $N$ . We consider that the total energy is conserved and given by

$$E \equiv \sum_i \left[ \frac{p_i^2}{2m_i} + u_i(s_i, n_i) \right] \quad (10)$$

while the total momentum

$$\mathbf{P} = \sum_i \mathbf{p}_i \quad (11)$$

is also a conserved quantity. We propose that the probability distribution of the system in the canonical ensemble is given by

$$P_{eq}(\{\mathbf{p}_i\}, \{\mathbf{r}_i\}, \{s_i\}) d\Gamma \sim e^{-\sum_i \left[ \frac{p_i^2}{2m_i} + u_i(s_i, n_i) - Ts_i \right] / (k_B T)} d\Gamma \quad (12)$$

where the state of the system is represented by a point in a  $7N$ -dimensional phase space  $\Gamma \equiv (\mathbf{p}_1, \dots, \mathbf{p}_N, \mathbf{r}_1, \dots, \mathbf{r}_N, s_1, \dots, s_N)$ . The function  $\mathcal{F}$ , defined as

$$\mathcal{F}(\{\mathbf{p}_i\}, \{\mathbf{r}_i\}, \{s_i\}; T) \equiv \sum_i \left[ \frac{p_i^2}{2m_i} + u_i(s_i, n_i) - Ts_i \right] \quad (13)$$

can be considered as a free energy functional of the system, and hence  $P_{eq}(\Gamma) \sim e^{-\mathcal{F}/(k_B T)}$ . Unlike the usual Hamiltonian of a conservative system,  $\mathcal{F}$  parametrically depends on the macroscopic temperature  $T$  set by the reservoir. Its dependence on the coordinates of the particles arises from the dependence of the local density in these coordinates, according to eq. (2),  $n_i = n(\{r_{ij}\})$ .

According to the definition in eq. (12),  $\theta_i$  is an estimator of the macroscopic system temperature

$$\langle \theta_i \rangle = \int d\Gamma \theta_i P_{eq}(\{\mathbf{p}_i\}, \{\mathbf{r}_i\}, \{s_i\}) = T \quad (14)$$

The choice given in eq. (12) is consistent with the probability distribution introduced in the energy form of the SDPD method<sup>40</sup>, although here we are working in the canonical ensemble.

### 2.3 Change in the independent variables

To complete our analysis, let us consider the effect on the mesoscopic properties when one set of independent (fluctuating) variables is changed into another set. In particular, consider the change from a set of  $s_i$  independent variables to a set of  $u_i$  independent variables, while keeping the system properties unchanged.

Let us consider that we introduce the new independent variables, and by virtue of eq. (6), we can then construct the function  $s_i(u_i, n_i)$ . Denoting  $\tilde{\Gamma} \equiv (\mathbf{p}_1, \dots, \mathbf{p}_N, \mathbf{r}_1, \dots, \mathbf{r}_N, u_1, \dots, u_N)$ , eq. (12) can then be written as

$$P_{eq}(\{\mathbf{p}_i\}, \{\mathbf{r}_i\}, \{s_i\}) d\Gamma \sim e^{-\sum_i \left[ \frac{p_i^2}{2m_i} + u_i - Ts_i(u_i, n_i) \right] / (k_B T)} \left| \frac{\partial \Gamma}{\partial \tilde{\Gamma}} \right| d\tilde{\Gamma} \quad (15)$$

The Jacobian of the transformation is  $|\partial \Gamma / \partial \tilde{\Gamma}| = (1/\theta_1)(1/\theta_2) \dots (1/\theta_N)$ . Hence, we can write

$$P_{eq}(\{\mathbf{p}_i\}, \{\mathbf{r}_i\}, \{u_i\}) d\tilde{\Gamma} \sim e^{-\sum_i \left[ \frac{p_i^2}{2m_i} + u_i - Tz_i(u_i, n_i) \right] / (k_B T)} d\tilde{\Gamma} \quad (16)$$

where we have introduced the *dressed particle entropy*<sup>53</sup>

$$z_i(u_i, n_i) \equiv s_i(u_i, n_i) - k_B \ln \frac{\theta_i(u_i, n_i)}{\theta_0} \quad (17)$$

Here *dressed*, in contrast to *bare*, refers to a quantity whose magnitude is affected by the fluctuations. In eq. (17), the temperature  $\theta_0 = 1$  is added for dimensional consistency, although its presence has no physical consequence. Note that the last term on the right-hand-side of eq. (17) is proportional to  $k_B$ , and corresponds to the

effect of the change of the nature of fluctuations from swapping the independent variable. We can thus define the free energy functional for the new set of independent variables, namely

$$\tilde{\mathcal{F}}(\{\mathbf{p}_i\}, \{\mathbf{r}_i\}, \{u_i\}; T) \equiv \sum_i \left[ \frac{p_i^2}{2m_i} + u_i - Tz_i(u_i, n_i) \right] \quad (18)$$

Introducing the dressed particle temperature  $\tau_i$  as

$$\frac{1}{\tau_i} \equiv \frac{\partial z_i}{\partial u_i} \Big|_{n_i} = \frac{1}{\theta_i} \left( 1 - k_B \frac{\partial \theta_i}{\partial u_i} \Big|_{n_i} \right) \quad (19)$$

we find that  $1/\tau_i$  is an appropriate estimator of the system temperature for the set of independent variables given by eq. (18), i.e.,

$$\left\langle \frac{1}{\tau_i} \right\rangle = \int d\tilde{\Gamma} \frac{1}{\tau_i} P_{eq}(\{\mathbf{p}_i\}, \{\mathbf{r}_i\}, \{z_i\}) = \frac{1}{T} \quad (20)$$

The relevance of these transformations will become more apparent when we define the entropy production at the mesoscopic level in Subsec. 3.2.

The function  $z$  plays an analogous role as  $s$ , although the 'intensive' variables are not the same in one representation as in the other. To see the differences, let us write  $u_i(z_i, n_i)$ , from which we obtain

$$du_i = \tau_i dz_i + \frac{\partial u_i}{\partial n_i} \Big|_{z_i} dn_i \quad (21)$$

where we have made use of eq. (19). Defining the particle heat capacity as

$$C_V \equiv \frac{\partial u_i}{\partial \theta_i} \Big|_{n_i} \quad (22)$$

we rewrite the relationship between bare and dressed temperatures in eq. (19) in a more significant form

$$\tau_i = \theta_i \frac{1}{1 - \frac{k_B}{C_V}} \quad (23)$$

At this point, it is convenient to introduce the particle equivalent of other usual derivatives such as the thermal expansion coefficient  $\alpha$

$$\alpha \equiv \frac{1}{n} \frac{\partial n}{\partial \theta} \Big|_{\pi} \quad (24)$$

together with the isothermal compressibility  $\beta$

$$\beta \equiv \frac{1}{n} \frac{\partial n}{\partial \pi} \Big|_{\theta} \quad (25)$$

With these definitions, after some algebra, one arrives at a more natural form for the second derivative in eq. (21)

$$\frac{\partial u}{\partial n} \Big|_{z} = \frac{\pi}{n^2} + \left[ \frac{k_B \tau}{C_V n^2} \alpha \right] \quad (26)$$

This expression gives rise to the definition of the *dressed pressure* of the particle, i.e.

$$\tilde{\pi} \equiv \pi + \frac{k_B \tau}{C_V} \alpha \quad (27)$$

so that

$$du_i = \tau_i dz_i + \frac{\tilde{\pi}_i}{n_i^2} dn_i \quad (28)$$

## 2.4 Models for the particle internal energy function

Up to this point in the derivation, we have introduced the formulation of the mesoscopic thermodynamics. Next, we propose a specific mesoscopic many-body force field based on an equation of state (MB-FF-EOS) that will be used later in the implementation of the generalised DPDE method. The intent of providing a specific MB-FF-EOS model here is for presentation clarity of the derivations that follow. In Appendix A, we provide other interesting forms of MB-FF-EOS models, including the Lennard-Jones (LJ) EOS that will be used for demonstrations of the generalised DPDE method.

### 2.4.1 Mesoscopic van der Waals many-body force field based on an equation of state

Let us consider that the particles satisfy a van der Waals-like mesoscopic MB-FF-EOS, namely

$$\pi = \frac{nk_B\theta}{1-bn} - an^2 \quad (29)$$

which depends on the particle temperature  $\theta$  and the local density  $n$ . The parameters  $a$  and  $b$  are the usual parameters in the van der Waals (vdW) EOS<sup>55</sup>.

Without loss of generality, we assume that eq. (29) is obtained after partial differentiation of a mesoscopic Helmholtz free energy defined by a Legendre transform of  $u(s, n)$ <sup>54</sup>

$$f(\theta, n) \equiv u - \theta s \Rightarrow df = -sd\theta + \left. \frac{\partial f}{\partial n} \right|_{\theta} dn \quad (30)$$

Note that no extensiveness at the mesoscopic level should be assumed thus far. In particular, note from eq. (13) that  $\mathcal{F} \neq \sum_i (p_i^2/m_i + f_i)$ . Therefore, eq. (30) should be interpreted only as a convenient mathematical transformation. The physical thermodynamic consequences are to be taken only from the behaviour of the ensemble of mesoscopic particles. Hence,

$$\begin{aligned} \pi &= \frac{nk_B\theta}{1-bn} - an^2 \\ &= n^2 \left. \frac{\partial f}{\partial n} \right|_{\theta} \end{aligned} \quad (31)$$

Integrating with respect to  $n$  one finds,

$$f = k_B\theta \ln\left(\frac{n}{1-bn}\right) - an + \Phi(\theta) \quad (32)$$

where  $\Phi(\theta)$  is an undefined function of the particle temperature. Focusing on the determination of the function  $u$  consistent with eq. (29), we have to introduce a second EOS for the DPDE particle, i.e.,

$$\begin{aligned} s &= - \left. \frac{\partial f}{\partial \theta} \right|_n \\ &= -k_B \ln\left(\frac{n}{1-bn}\right) - \Phi'(\theta) \end{aligned} \quad (33)$$

The internal energy can then be readily obtained as

$$\begin{aligned} u &= f + \theta s \\ &= \Phi(\theta) - \theta\Phi'(\theta) - an \end{aligned} \quad (34)$$

According to the classical DPDE model with a constant heat capacity per particle  $C_V$ , one writes  $C_V = \left. \frac{\partial u}{\partial \theta} \right|_n = -\theta\Phi''(\theta)$ , which implies

$$\Phi(\theta) = -C_V \theta(\ln\theta - 1) + c_1\theta + c_2 \quad (35)$$

where  $c_1$  and  $c_2$  are arbitrary constants. Thus, the internal energy is

$$u = C_V\theta - an - c_2 \quad (36)$$

We arbitrarily choose  $c_1 = 0$  and  $c_2 = 0$ , to recover the original model for the DPDE particles. However, we will write  $c_1 = C_V \ln\theta_0$  with  $\theta_0 = 1$  for dimensional consistency of eq. (35). From eq. (36) we obtain  $\theta = (u + an)/C_V$ , and arrive at one of the central functions of the problem, namely

$$s(u, n) = -k_B \ln\left(\frac{n}{1-bn}\right) + C_V \ln\left(\frac{u+an}{C_V\theta_0}\right) \quad (37)$$

This function can be inverted to obtain the sought result

$$u(s, n) = C_V\theta_0 e^{s/C_V} \left(\frac{n}{1-bn}\right)^{k_B/C_V} - an \quad (38)$$

It is also interesting to provide the expression for the dressed particle entropy  $z$ . Effectively, in view of eq. (17) and eq. (37), one finds

$$z(u, n) = -k_B \ln\left(\frac{n}{1-bn}\right) + (C_V - k_B) \ln\left(\frac{u+an}{C_V\theta_0}\right) \quad (39)$$

We also provide here the expressions for the excess internal energy and entropy of the vdW EOS, as these equations were used in ref.<sup>34</sup> based on an excess pressure

$$\frac{\pi^{ex}}{n^2} = \frac{bk_B\theta}{1-bn} - a \quad (40)$$

Employing a constant heat capacity for the model, we can write

$$u(s, n) \equiv u^{ex}(s, n) = C_V\theta_0 e^{s/C_V} \left(\frac{1}{1-bn}\right)^{k_B/C_V} - an \quad (41)$$

The entropy function is then

$$s(u, n) \equiv s^{ex}(u, n) = -k_B \ln\left(\frac{1}{1-bn}\right) + C_V \ln\left(\frac{u+an}{C_V\theta_0}\right) \quad (42)$$

### 2.4.2 General form for systems with linear dependence in the particle temperature

The vdW pressure defined by eq. (29) can be generalised considering that the pressure may be density dependent, while its particle temperature dependence still remains linear. Within these conditions, the general form of the mesoscopic MB-FF-EOS depends upon two functions of  $n$  alone, denoted by  $\psi(n)$  and  $\mathcal{V}(n)$ , where  $u$  can be written as

$$u(s, n) = C_V\theta_0 e^{s/C_V} \psi(n)^{k_B/C_V} + \mathcal{V}(n) \quad (43)$$

The general equation for the particle pressure takes the form

$$\pi = k_B \theta \frac{n^2 \psi'(n)}{\psi(n)} + n^2 \mathcal{V}'(n) \quad (44)$$

The entropy function is then

$$s(u, n) = C_V \ln \left[ \frac{u - \mathcal{V}(n)}{C_V \theta_0} \right] - k_B \ln \psi(n) \quad (45)$$

while the dressed particle entropy takes the form

$$z(u, n) = (C_V - k_B) \ln \left[ \frac{u - \mathcal{V}(n)}{C_V \theta_0} \right] - k_B \ln \psi(n) \quad (46)$$

### 3 Dynamic equations

#### 3.1 Reversible interactions

Let us consider that with respect to the reversible interactions,  $\mathcal{F}$  acts as a generalised Hamiltonian, such that

$$\dot{\mathbf{r}}_i = \frac{\mathbf{p}_i}{m_i} \quad (47)$$

$$\dot{\mathbf{p}}_i = - \sum_{j \neq i} \left. \frac{\partial u_j}{\partial n_j} \right|_{s_j} \frac{\partial n_j}{\partial \mathbf{r}_i} \equiv \mathbf{f}_i^C \quad (48)$$

$$\dot{s}_i = 0 \quad (49)$$

With this choice,  $\dot{\mathcal{F}} = 0$ . While the interpretation of eq. (47) is straightforward, eq. (48) deserves further comment. Due to translational invariance of the system, the set of functions  $u_i$  is independent of an arbitrary variation  $\boldsymbol{\lambda}$  of the origin of coordinates. In other words, transforming  $\mathbf{r}_i \rightarrow \mathbf{r}_i + \boldsymbol{\lambda}$  leaves  $n_i$  invariant, as well as then the internal energy. Therefore,

$$\frac{\partial n_i}{\partial \boldsymbol{\lambda}} = 0 \Rightarrow \sum_j \frac{\partial n_i}{\partial \mathbf{r}_j} = 0$$

Furthermore, we can write

$$\sum_j \left. \frac{\partial u_j}{\partial n_j} \right|_{s_j} \frac{\partial n_j}{\partial \mathbf{r}_i} = \sum_{j \neq i} \left( \left. \frac{\partial u_j}{\partial n_j} \right|_{s_j} \frac{\partial n_j}{\partial \mathbf{r}_i} - \left. \frac{\partial u_i}{\partial n_i} \right|_{s_i} \frac{\partial n_i}{\partial \mathbf{r}_j} \right)$$

and by using

$$\frac{\partial n_i}{\partial \mathbf{r}_j} = - \frac{\partial n_j}{\partial \mathbf{r}_i} = - \frac{w'(r_{ij})}{[w]} \mathbf{e}_{ij}$$

for  $j \neq i$ , we arrive at

$$\mathbf{f}_i^C = \sum_{j \neq i} \mathbf{f}_{ij}^C = - \sum_{j \neq i} \left( \left. \frac{\partial u_j}{\partial n_j} \right|_{s_j} + \left. \frac{\partial u_i}{\partial n_i} \right|_{s_i} \right) \frac{w'_{ij}}{[w]} \mathbf{e}_{ij} \quad (50)$$

Note that the form of the force corresponds to the one related to compression-expansion of the particle under adiabatic conditions. Finally, let us introduce the particle pressure to the force expression (50) by using eq. (7)

$$\mathbf{f}_{ij}^C = - \left( \frac{\pi_i}{n_i^2} + \frac{\pi_j}{n_j^2} \right) \frac{w'_{ij}}{[w]} \mathbf{e}_{ij} \quad (51)$$

Angular momentum is also preserved by eq. (51), moreover, it is formally identical to the expression used in SDPD<sup>40</sup>, yet here ob-

tained bottom-up, from the properties of an ensemble of particles defined *a priori*. Notice, however, that the particle pressure is not exactly the macroscopic pressure of the ensemble. For instance, using the virial as an estimator of the system (macroscopic) pressure, we obtain

$$P \equiv \frac{1}{DV} \left\langle \sum_i \frac{p_i^2}{m_i} + \sum_i \sum_{j < i} \mathbf{r}_{ij} \cdot \mathbf{f}_{ij}^C \right\rangle \quad (52)$$

which using eq. (51) can also be written as

$$P = \frac{Nk_B T}{V} + \left\langle \sum_i \sum_{j < i} \left( \frac{\pi_i}{n_i^2} + \frac{\pi_j}{n_j^2} \right) \frac{r_{ij} w'_{ij}}{[w]} \right\rangle \quad (53)$$

It is clear from eq. (53) that the macroscopic pressure of the system differs from the functional form of the particle pressure, precisely due to the fluctuations that couple all the fluctuating variables in the average. Therefore, as noted by Pagonabarraga and Frenkel<sup>34</sup>, the particle pressure acts as an *excess* pressure and not as a *total* pressure of the system, as it is used in SDPD. Only close to the macroscopic limit, where the fluctuations are negligible<sup>40</sup>, is the total pressure approximately the particle pressure. In practice then, when implementing the generalised DPDE method, the excess pressure determined from the analytical EOS is used to determine the particle pair forces, as opposed to using the total pressure.

Finally, eq. (49) is an adiabatic condition that indicates that no heat is exchanged between the internal degrees-of-freedom of the particles, neither amongst themselves nor with the reservoir in a reversible transformation. The variation of the particle internal energy is then only due to the expansion-compression work resulting from the conservative forces given by eq. (51).

#### 3.2 Irreversible interactions

In the absence of fluctuations, the dynamics of the system is driven by the condition of minimum of  $\mathcal{F}$ , i.e.  $\dot{\mathcal{F}} < 0$ . We will not define the equation for the time dependence of the entropy yet, but we introduce the dissipative forces into the equation for the momentum, eq. (48), leaving the variation of the position unchanged with respect to eq. (47), i.e.

$$\dot{\mathbf{p}}_i = - \sum_{j \neq i} \left. \frac{\partial u_j}{\partial n_j} \right|_{s_j} \frac{\partial n_j}{\partial \mathbf{r}_i} \equiv \mathbf{f}_i^C + \mathbf{f}_i^D \quad (54)$$

Writing  $\dot{\mathcal{F}}$  in terms of the dynamic quantities one has

$$\dot{\mathcal{F}} = \sum_i \left( \frac{\mathbf{p}_i}{m_i} \cdot \dot{\mathbf{p}}_i + \theta_i \dot{s}_i - \mathbf{f}_i^C \cdot \dot{\mathbf{r}}_i - T \dot{s}_i \right) < 0 \quad (55)$$

Then, replacing the dynamic equations the latter takes the form

$$\dot{\mathcal{F}} = \sum_i \left( \mathbf{f}_i^D \cdot \frac{\mathbf{p}_i}{m} + \theta_i \dot{s}_i - T \dot{s}_i \right) < 0 \quad (56)$$

From eq. (9), and assuming that  $\dot{W}_i^{irrev} = -\mathbf{f}_i^D \cdot \frac{\mathbf{p}_i}{m}$ , one arrives at the expression

$$\dot{\mathcal{F}} = \sum_i (\dot{q}_i - T \dot{s}_i) < 0 \quad (57)$$

The total heat transferred by particle  $i$  can be separated in different contributions, involving the interparticle heat exchange as well as the heat exchange with the external reservoir

$$\dot{q}_i = \sum_{j \neq i} \dot{q}_{ij} + \dot{Q}_i \quad (58)$$

The interparticle heat exchange satisfies  $\dot{q}_{ij} = -\dot{q}_{ji}$  due to energy conservation. Hence, the summation over all the particles is zero. Introducing this definition into eq. (57), one finds

$$\mathcal{F} = \sum_i (\dot{Q}_i - T \dot{s}_i) < 0 \quad (59)$$

or, what is the same

$$\sum_i \dot{s}_i > \sum_i \frac{\dot{Q}_i}{T} \quad (60)$$

As  $-\sum_i \dot{Q}_i/T$  is the entropy variation of the reservoir, this equation indicates the obvious result that the inner processes in the system should lead to a positive entropy production. In other words, if we split the particle entropy production into an internal  $s_i^{int}$  and an external  $s_i^{ext}$  contributions, the latter being related to the heat exchanged with the reservoir, eq. (60) in fact simply indicates that

$$\sum_i s_i^{int} > 0 \quad (61)$$

To provide then an indication of the entropy production at the particle level, let us consider again eq. (9), which in terms of the internal entropy production reads

$$\theta_i s_i^{int} = \sum_{j \neq i} \dot{q}_{ij} + \dot{W}_i^{irrev} \quad (62)$$

On the one hand, from the definition of the irreversible work done on the particle indicated above, we demand that

$$\dot{W}_i^{irrev} = -\mathbf{f}_i^D \cdot \frac{\mathbf{p}_i}{m} > 0 \quad (63)$$

Invoking pairwise additiveness and momentum conservation, it follows that  $\mathbf{f}_i^D = \sum_{j \neq i} \mathbf{f}_{ij}^D$ , with  $\mathbf{f}_{ij}^D = -\mathbf{f}_{ji}^D$ . Then, we can straightforwardly demand that

$$\dot{W}_i^{irrev} = -\mathbf{f}_i^D \cdot \frac{\mathbf{p}_i}{m} = -\sum_{j < i} (\mathbf{v}_i - \mathbf{v}_j) \cdot \mathbf{f}_{ij}^D > 0 \quad (64)$$

The usual form for the dissipative force in DPD complies with this requirement and will be used along this article, i.e.

$$\mathbf{f}_{ij}^D = -\gamma_{ij} \mathbf{e}_{ij} \mathbf{e}_{ij} \cdot (\mathbf{v}_i - \mathbf{v}_j) \quad (65)$$

where the friction kernel is

$$\gamma_{ij} \equiv \gamma \omega^2 \left( \frac{r_{ij}}{R_{cut}^D} \right) \quad (66)$$

The kernel  $\gamma_{ij}$  is a function of only the interparticle distance in order to preserve Galilean invariance, while it is symmetric under the permutation of their indices, in order to maintain total momentum and energy conservation. Furthermore, since the dissipative force is directed along the line of the particle centres, the angular momentum is also preserved by the dissipative force

expression. In this expression,  $R_{cut}^D$  stands for the radius of interaction of the dissipative force.

On the other hand, from eqs. (5) and (28) it follows that at constant volume,

$$\tau_i z_i^{int} |_{n_i} = \theta_i s_i^{int} |_{n_i} = \sum_{j \neq i} \dot{q}_{ij} \quad (67)$$

Aiming at using the internal energy as independent variable in the algorithm, we will demand that

$$z_i^{int} |_{n_i} = \frac{\theta_i}{\tau_i} s_i^{int} |_{n_i} = \sum_{j \neq i} \frac{1}{\tau_i} \dot{q}_{ij} > 0 \quad (68)$$

As  $\theta_i/\tau_i$  is always positive, with this choice  $s_i^{int} |_{n_i} > 0$  is also guaranteed. Using the fact that  $\dot{q}_{ij} = -\dot{q}_{ji}$ , we can write

$$z_i^{int} |_{n_i} = \sum_{j < i} \left( \frac{1}{\tau_i} - \frac{1}{\tau_j} \right) \dot{q}_{ij} > 0 \quad (69)$$

According to<sup>20,56</sup>, to assure the positiveness of the entropy production, we demand that

$$\dot{q}_{ij} = -\kappa_{ij} \left( \frac{1}{\tau_j} - \frac{1}{\tau_i} \right) \quad (70)$$

The heat exchange kernel  $\kappa_{ij}$  is a function of the interparticle distance, which we express as

$$\kappa_{ij} = \kappa \bar{\omega}^2 \left( \frac{r_{ij}}{R_{cut}} \right) \quad (71)$$

where  $\bar{\omega}$  is a weight function depending on the distance between particles, and  $R_{cut}$  is the characteristic distance for the heat exchange.  $\kappa$  is a coefficient modulating the heat conductivity of the system. The kernel satisfies Galilean invariance.

In analogy with eq. (70) we also introduce the equation for the interaction of the particles with the heat reservoir, namely,

$$\dot{Q}_i = -\kappa_i \left( \frac{1}{T} - \frac{1}{\tau_i} \right) \quad (72)$$

where the kernel  $\kappa_i$  is analogous to the interparticle kernel given in eq. (71).

To end this section, some important comments are in order. On one hand, we have used  $\mathcal{F}$  in eq. (13), with a given choice of the independent variables, as a generalised Hamiltonian from which we have derived the dynamic equations of motion (ignoring the fluctuations). The function  $\mathcal{F}$  cannot be equivalently used to obtain the same equations of motion as it incorporates effects of the change of description, which are related to the finite size of the mesoparticles and the fluctuating nature of their variables. The choice of the generalised Hamiltonian associates the *systematic* dynamics with the saddle point of the probability distribution in eq. (15). However, this saddle point analysis of the equivalent distribution in eq. (16) yields different non-equivalent systematic dynamics.

On the other hand, the form given in eq. (70) relating the interparticle heat transport with the inverse dressed temperatures is a matter of choice. Instead, one could have defined this quantity

in terms of the difference of inverse bare temperatures. However, our choice assures that the average of the dissipative interactions vanishes in equilibrium, in view of eq. (20), which would be not the case if the bare temperatures were used instead.

## 4 The generalised DPDE algorithm

### 4.1 Dynamic equations

Following the previous definitions and the analysis of the thermodynamics at the mesoscopic level, we can propose the algorithm for the generalised DPDE method. Here we use the original DPDE perspective<sup>20</sup>, which is centred on the particle internal energy  $u_i$  as the dynamic variable instead of  $s_i$ , as it is usually done in SDPD<sup>39</sup>. An exception is the energy form of SDPD given in ref.<sup>40</sup>, however that formulation does not consider the heat flow. We propose that positions and velocities are varied according to

$$\mathbf{r}_i' = \mathbf{r}_i + \frac{\mathbf{p}_i}{m_i} \delta t \quad (73)$$

$$\mathbf{p}_i' = \mathbf{p}_i + \sum_{j \neq i} \mathbf{f}_{ij}^C \delta t + \sum_{j \neq i} \mathbf{f}_{ij}^D \delta t + \sum_{j \neq i} \delta \mathbf{p}_{ij}^R \quad (74)$$

where prime and non-prime variables refer to the time  $t + \delta t$  and  $t$ , respectively,  $\delta t$  is the time step, and the conservative and dissipative forces,  $\mathbf{f}_{ij}^C$  and  $\mathbf{f}_{ij}^D$ , are defined in eqs. (51) and (65), respectively. The random contribution to the momentum is given by

$$\begin{aligned} \delta \mathbf{p}_{ij}^R &= \sqrt{k_B(\theta_i + \theta_j)} \gamma_{ij} \xi_{ij} \mathbf{e}_{ij} \delta t^{1/2} \\ &= \sigma_{ij} \xi_{ij} \mathbf{e}_{ij} \delta t^{1/2} \end{aligned} \quad (75)$$

with  $\delta \mathbf{p}_{ij}^R = -\delta \mathbf{p}_{ji}^R$ . In eq. (75),

$$\sigma_{ij} = \sqrt{k_B(\theta_i + \theta_j)} \gamma_{ij} \quad (76)$$

and the normalised Gaussian random numbers  $\xi_{ij}$  satisfy

$$\begin{aligned} \langle \xi_{ij} \rangle &= 0 \\ \langle \xi_{ij} \xi_{kl} \rangle &= \delta_{ik} \delta_{jl} - \delta_{il} \delta_{jk} \end{aligned}$$

where the average is taken over the probability distribution of  $\xi_{ij}$ . Eq. (76) represents the fluctuation-dissipation theorem, which is derived in Appendix B [see eq. (123)]. Note that the functional form in eq. (76) is different from the original DPDE method<sup>20</sup>, where the temperature scales as  $(\theta_i + \theta_j)$ , rather than  $\tau_i \tau_j / (\tau_i + \tau_j)$ . This different temperature scaling is due to the difference between the dynamics constructed from  $\mathcal{F}$  as a generalised Hamiltonian instead of  $\tilde{\mathcal{F}}$ , as was done in the original DPDE formulation<sup>20</sup>.

The third equation defining the algorithm of the generalised DPDE method refers to the dynamics of the particle internal energy  $u_i$ , which can be related to a conservation law, unlike the bare or dressed particle entropy. Thus, after having defined the equations governing the changes in the positions and momenta, we can derive the non-fluctuating part of the particle internal energy variation from the balance of the total energy of the system.

Hence, for a system in contact with an energy reservoir at fixed volume, we can establish from eq. (10) that

$$\sum_i \left( \frac{p_i'^2}{2m_i} - \frac{p_i^2}{2m_i} + u_i' - u_i \right) = \Delta E \quad (77)$$

with  $\Delta E$  taken as the energy exchanged with the heat source. Using eq. (74), and retaining terms up to order  $\mathcal{O}(\delta t)$ , one has

$$\begin{aligned} u_i' &= u_i + \frac{1}{2} \sum_{j \neq i} (\mathbf{v}_i - \mathbf{v}_j) \cdot \mathbf{e}_{ij} \gamma_{ij} \mathbf{e}_{ij} \cdot (\mathbf{v}_i - \mathbf{v}_j) \delta t \\ &\quad - \frac{1}{2} \sum_{j \neq i} (\mathbf{v}_i - \mathbf{v}_j) \cdot \mathbf{f}_{ij}^C \delta t - \frac{1}{2} \sum_{j \neq i} (\mathbf{v}_i - \mathbf{v}_j) \cdot \delta \mathbf{p}_{ij}^R \\ &\quad - \frac{1}{2m_i} \sum_{j \neq i} \sum_{l \neq i} \delta \mathbf{p}_{ij}^R \cdot \delta \mathbf{p}_{il}^R + \dot{q}_i \delta t + \sum_{j \neq i} \delta u_{ij}^R \end{aligned} \quad (78)$$

where  $\delta u_{ij}^R$  is the random heat exchanged between particles  $i$  and  $j$  during the time step  $\delta t$ . Due to total energy conservation, we require that  $\delta u_{ij}^R = -\delta u_{ji}^R$ . In eq. (78), note the term proportional to  $\delta \mathbf{p}_{ij}^R \cdot \delta \mathbf{p}_{il}^R$ . According to eq. (75), eq. (78) is of  $\mathcal{O}(\delta t)$ , but is usually replaced by its equilibrium average when the approximation based on the Fokker-Planck equation is used. The presence of this term allows for an energy conservation up to  $\mathcal{O}(\delta t)$  at every time step, and not simply of its average. In defining the above equation, the energy exchanged with the reservoir can only be given by the heat transferred as the volume of the system is held fixed, i.e.,

$$\Delta E = \sum_i \dot{Q}_i \delta t \quad (79)$$

Following the original DPDE formalism, the random contribution to the particle internal energy is defined as<sup>20</sup>

$$\begin{aligned} \delta u_{ij}^R &= \sqrt{2k_B \kappa_{ij}} \bar{\xi}_{ij} \delta t^{1/2} \\ &= \alpha_{ij} \bar{\xi}_{ij} \delta t^{1/2} \end{aligned} \quad (80)$$

where

$$\alpha_{ij} = \sqrt{2k_B \kappa_{ij}} \quad (81)$$

and the normalised Gaussian number  $\bar{\xi}_{ij}$  satisfies the properties

$$\begin{aligned} \langle \bar{\xi}_{ij} \rangle &= 0 \\ \langle \bar{\xi}_{ij} \bar{\xi}_{kl} \rangle &= \delta_{ik} \delta_{jl} - \delta_{il} \delta_{jk} \end{aligned}$$

Here, the average is taken over the probability distribution of  $\bar{\xi}_{ij}$ . The fluctuation-dissipation theorem given by eq. (81) can also be obtained by the standard methods<sup>57</sup>.

In summary, the EOM for the positions, momenta, and particle internal energy in the generalised DPDE method are given by eqs. (73), (74), and (78), respectively, with the random contribution to the momentum and the particle internal energy,  $\delta \mathbf{p}_{ij}^R$  and  $\delta u_{ij}^R$ , defined in eqs. (75) and (80), respectively, and the friction and heat exchange kernels,  $\gamma_{ij}$  and  $\kappa_{ij}$ , given by eqs. (66) and (71), respectively.

## 4.2 Numerical discretisation

The integration of the EOM was performed using the extended Shardlow splitting algorithm (eSSA)<sup>26</sup>. The eSSA splits the integration into reversible and irreversible terms with the overall solution operator,  $\Phi_{\delta t}$ , given as<sup>49</sup>

$$\Phi_{\delta t} \simeq \Phi_{\delta t;1,2}^{irrev} \circ \Phi_{\delta t;1,3}^{irrev} \circ \dots \circ \Phi_{\delta t;i,j}^{irrev} \circ \dots \circ \Phi_{\delta t;N-2,N}^{irrev} \circ \Phi_{\delta t;N-1,N}^{irrev} \circ \Phi_{\delta t}^{rev} \quad (82)$$

The reversible term  $\Phi_{\delta t}^{rev}$  corresponds to

$$\begin{aligned} d\mathbf{r}_i &= \frac{\mathbf{p}_i}{m_i} \delta t \quad (i = 1, \dots, N) \\ d\mathbf{p}_i &= \mathbf{f}_i^C \delta t \\ du_i &= -\frac{1}{2} \sum_{j \neq i} \mathbf{v}_{ij} \cdot \mathbf{f}_{ij}^C \delta t \end{aligned} \quad (83)$$

where  $\mathbf{f}_i^C$  and  $\mathbf{f}_{ij}^C$  are given by eqs. (50) and (51), respectively, and  $\mathbf{v}_{ij} \equiv \mathbf{v}_i - \mathbf{v}_j = \frac{\mathbf{p}_i}{m_i} - \frac{\mathbf{p}_j}{m_j}$ .

The reversible term  $\Phi_{\delta t}^{rev}$  is discretised using the velocity-Verlet algorithm as<sup>58</sup>

$$\begin{aligned} \mathbf{p}_i \left( t + \frac{\delta t}{2} \right) &= \mathbf{p}_i(t) + \frac{\delta t}{2} \mathbf{f}_i^C(t) \quad (i = 1, \dots, N) \\ \mathbf{r}_i(t + \delta t) &= \mathbf{r}_i(t) + \delta t \frac{\mathbf{p}_i \left( t + \frac{\delta t}{2} \right)}{m_i} \\ u_i \left( t + \frac{\delta t}{2} \right) &= u_i(t) - \frac{\delta t}{4} \sum_{j \neq i} \mathbf{v}_{ij}(t) \cdot \mathbf{f}_{ij}^C(t) \end{aligned} \quad (84)$$

evaluate:  $\left\{ \mathbf{f}_i^C(t + \delta t) \right\}_{i=1}^N$

$$\mathbf{p}_i(t + \delta t) = \mathbf{p}_i \left( t + \frac{\delta t}{2} \right) + \frac{\delta t}{2} \mathbf{f}_i^C(t + \delta t) \quad (i = 1, \dots, N)$$

evaluate:  $\left\{ \sum_{j \neq i} \mathbf{v}_{ij}(t + \delta t) \cdot \mathbf{f}_{ij}^C(t + \delta t) \right\}_{i=1}^N$

$$u_i(t + \delta t) = u_i \left( t + \frac{\delta t}{2} \right) - \frac{\delta t}{4} \sum_{j \neq i} \mathbf{v}_{ij}(t + \delta t) \cdot \mathbf{f}_{ij}^C(t + \delta t) \quad (i = 1, \dots, N)$$

Each irreversible term  $\Phi_{\delta t;i,j}^{irrev}$  then corresponds to

$$\begin{aligned} d\mathbf{p}_i^{i-j} &= \mathbf{f}_{ij}^{D,i-j} \delta t + \delta \mathbf{p}_{ij}^{R,i-j} \\ d\mathbf{p}_j^{i-j} &= -d\mathbf{p}_i^{i-j} \\ du_i^{i-j} &= -\frac{\mathbf{v}_{ij}^{i-j}}{2} \cdot \left( \mathbf{f}_{ij}^{D,i-j} \delta t + \delta \mathbf{p}_{ij}^{R,i-j} \right) + q_{ij}^{i-j} \delta t + \delta u_{ij}^{R,i-j} \\ du_j^{i-j} &= -\frac{\mathbf{v}_{ij}^{i-j}}{2} \cdot \left( \mathbf{f}_{ij}^{D,i-j} \delta t + \delta \mathbf{p}_{ij}^{R,i-j} \right) - q_{ij}^{i-j} \delta t - \delta u_{ij}^{R,i-j} \end{aligned} \quad (85)$$

As shown in Ref.<sup>26</sup>, the equations for  $du_i^{i-j}$  and  $du_j^{i-j}$  can be re-

written as

$$\begin{aligned} du_i^{i-j} &= -\frac{1}{2} d \left( \frac{\mathbf{p}_i^{i-j} \cdot \mathbf{p}_i^{i-j}}{2m_i} + \frac{\mathbf{p}_j^{i-j} \cdot \mathbf{p}_j^{i-j}}{2m_j} \right) \\ &\quad + q_{ij}^{i-j} \delta t + \delta u_{ij}^{R,i-j} \\ du_j^{i-j} &= -\frac{1}{2} d \left( \frac{\mathbf{p}_i^{i-j} \cdot \mathbf{p}_i^{i-j}}{2m_i} + \frac{\mathbf{p}_j^{i-j} \cdot \mathbf{p}_j^{i-j}}{2m_j} \right) \\ &\quad - q_{ij}^{i-j} \delta t - \delta u_{ij}^{R,i-j} \end{aligned} \quad (86)$$

where the superscript  $i-j$  indicates that the variation of momenta and particle internal particle energy is considered for a pair of interaction particles  $i$  and  $j$  only;  $\mathbf{f}_{ij}^{D,i-j}$ ,  $\mathbf{p}_{ij}^{R,i-j}$ ,  $q_{ij}^{i-j}$ , and  $\delta u_{ij}^{R,i-j}$  are given by eqs. (65), (75), (70), and (80), respectively.

Each irreversible term  $\Phi_{\delta t;i,j}^{irrev}$  can also be discretised using the velocity-Verlet algorithm as<sup>26</sup>

$$\begin{aligned} \mathbf{p}_i \left( t + \frac{\delta t}{2} \right) &= \mathbf{p}_i(t) - \frac{\delta t}{2} \gamma_{ij} \mathbf{v}_{ij}(t) \cdot \mathbf{e}_{ij} \mathbf{e}_{ij} + \frac{\delta t^{1/2}}{2} \sigma_{ij} \xi_{ij} \mathbf{e}_{ij} \\ \mathbf{p}_j \left( t + \frac{\delta t}{2} \right) &= \mathbf{p}_j(t) + \frac{\delta t}{2} \gamma_{ij} \mathbf{v}_{ij}(t) \cdot \mathbf{e}_{ij} \mathbf{e}_{ij} - \frac{\delta t^{1/2}}{2} \sigma_{ij} \xi_{ij} \mathbf{e}_{ij} \\ \mathbf{p}_i(t + \delta t) &= \mathbf{p}_i \left( t + \frac{\delta t}{2} \right) - \frac{\delta t}{2} \frac{\gamma_{ij}}{1 + \frac{\mu_{ij}}{2} \gamma_{ij} \delta t} \left\{ \mathbf{v}_{ij} \left( t + \frac{\delta t}{2} \right) \cdot \mathbf{e}_{ij} \mathbf{e}_{ij} \right. \\ &\quad \left. + \delta t^{1/2} \frac{\mu_{ij}}{2} \sigma_{ij} \xi_{ij} \mathbf{e}_{ij} \right\} + \frac{\delta t^{1/2}}{2} \sigma_{ij} \xi_{ij} \mathbf{e}_{ij} \\ \mathbf{p}_j(t + \delta t) &= \mathbf{p}_j \left( t + \frac{\delta t}{2} \right) + \frac{\delta t}{2} \frac{\gamma_{ij}}{1 + \frac{\mu_{ij}}{2} \gamma_{ij} \delta t} \left\{ \mathbf{v}_{ij} \left( t + \frac{\delta t}{2} \right) \cdot \mathbf{e}_{ij} \mathbf{e}_{ij} \right. \\ &\quad \left. + \delta t^{1/2} \frac{\mu_{ij}}{2} \sigma_{ij} \xi_{ij} \mathbf{e}_{ij} \right\} - \frac{\delta t^{1/2}}{2} \sigma_{ij} \xi_{ij} \mathbf{e}_{ij} \\ u_i(t + \delta t) &= u_i(t) - \frac{1}{2} \left[ \frac{\mathbf{p}_i(t + \delta t) \cdot \mathbf{p}_i(t + \delta t)}{2m_i} + \frac{\mathbf{p}_j(t + \delta t) \cdot \mathbf{p}_j(t + \delta t)}{2m_j} \right. \\ &\quad \left. - \frac{\mathbf{p}_i(t) \cdot \mathbf{p}_i(t)}{2m_i} - \frac{\mathbf{p}_j(t) \cdot \mathbf{p}_j(t)}{2m_j} \right] + \delta t \kappa_{ij} \left( \frac{1}{\tau_i} - \frac{1}{\tau_j} \right) + \delta t^{1/2} \alpha_{ij} \bar{\xi}_{ij} \\ u_j(t + \delta t) &= u_j(t) - \frac{1}{2} \left[ \frac{\mathbf{p}_i(t + \delta t) \cdot \mathbf{p}_i(t + \delta t)}{2m_i} + \frac{\mathbf{p}_j(t + \delta t) \cdot \mathbf{p}_j(t + \delta t)}{2m_j} \right. \\ &\quad \left. - \frac{\mathbf{p}_i(t) \cdot \mathbf{p}_i(t)}{2m_i} - \frac{\mathbf{p}_j(t) \cdot \mathbf{p}_j(t)}{2m_j} \right] - \delta t \kappa_{ij} \left( \frac{1}{\tau_i} - \frac{1}{\tau_j} \right) - \delta t^{1/2} \alpha_{ij} \bar{\xi}_{ij} \end{aligned} \quad (87)$$

where  $\mu_{ij} = \frac{1}{m_i} + \frac{1}{m_j}$ , and the superscript  $i-j$  has been omitted for notational simplicity. The temperatures  $\theta_i$ ,  $\theta_j$ ,  $\tau_i$  and  $\tau_j$  are updated with the mesoscopic MB-FF-EOS using the updated particle internal energies, before these equations are applied to another pair of particles.

For this algorithm, it is important to note that the integration of the irreversible terms exactly conserves the total energy  $E$  at each time step. However, analogous to an application of the velocity-Verlet algorithm in microcanonical molecular dynamics, the integration of the reversible term does not conserve  $E$  at each time

step. Rather, the symplectic velocity-Verlet algorithm preserves  $E$  only up to terms of order  $\delta t^2$ , conserving a pseudo-Hamiltonian that differs from the true Hamiltonian by this difference of order  $\delta t^2$ . Although there is long-time stability for the velocity-Verlet algorithm in conservative systems, this energy fluctuation gives rise to an energy drift when coupled with dissipative processes, as in the DPDE-type algorithms<sup>26</sup>.

### 4.3 Computational details

For validation of the generalised DPDE method, analytical EOSs for the LJ and vdW fluids were considered. The LJ EOS developed by Kolafa and Nezbeda was implemented<sup>59</sup>, which produces results of high accuracy for both the pressure and internal energy over a wide range of temperatures and densities. The LJ EOS is used for most of the validation tests presented here, including the non-equilibrium simulation scenarios of flash heating response and fluid phase separation. Other validation tests are performed using the vdW EOS<sup>34,55,60</sup>. For both fluid models, the following parameters for argon (molar mass of 39.948 g/mol) were used:  $\sigma_{\text{LJ}} = 3.35654 \text{ \AA}$  and  $\epsilon_{\text{LJ}}/k_B = 291.382 \text{ K}$ ;  $a_{\text{vdW}} = 27197.659 \text{ K\AA}^3$  and  $b_{\text{vdW}} = 53.48 \text{ \AA}^3$ . All data is presented in reduced units, based on these LJ parameters.

A quadratic weighting function was used in the local density model, while the typical weighting function  $(1 - r/R_{\text{cut}})$  was used for the friction kernel  $\omega(r)$ , eq. 66, and the heat exchange kernel  $\bar{\omega}(r)$ , eq. 71, where  $R_{\text{cut}} = R_{\text{cut}}^D = \bar{R}_{\text{cut}} = 4$ . Note that other choices of weighting functions are possible, e.g., the Lucy function<sup>37</sup>, popular in SPH and SDPD simulations, a third order spline function, or a smoothed step function<sup>52</sup>.

For all of the results presented, the following simulation parameters were used unless stated otherwise:  $N = 27,000$ ;  $\delta t = 0.01$  (corresponding to 13.63 fs in real units);  $C_V = 60$ ;  $\gamma = 4.5$ ;  $\kappa = 1$ . A range of state points were considered:  $T = 1$  to 3 and  $\rho \equiv N/V = 0.2$  to 0.8, which spans both liquid and supercritical fluid phase behaviour. For initialisation, particles were placed on a simple cubic lattice structure in a cubic simulation box that was appropriately sized to the target densities, then simulated for an equilibration period of  $5 \times 10^5$  time steps. After equilibration, the systems were simulated for an additional  $5 \times 10^5$  time steps from which the average thermodynamic properties were determined by collecting data every 50 time steps. All simulations were conducted using the LAMMPS software package<sup>61</sup>, except for the isothermal DPD simulations presented in Sec. 5.1, where an in-house code was used.

Finally, when using the vdW EOS as a many-body force field, a scheme that prevents numerical instabilities at low and high local densities has been introduced. To prevent compression of the fluid below the excluded volume, the scheme ensures that a local density of a particle is not higher than a specified threshold, thus avoiding numerical issues associated with unphysical compression. Similarly, to avoid numerical instabilities at very low local densities, a minimum threshold of  $10^{-6}$  is enforced. Details of the scheme can be found in Supplemental Material A.

## 5 Results and Discussion

### 5.1 Validation of the generalised DPDE method

For validation of the generalised DPDE method, the particle probability distributions were analysed (Fig. 1). The particle probability distributions of the particle internal energy, particle temperature, particle momenta and local density were determined from the generalised DPDE method for the vdW EOS at  $T = 1.5$  and  $\rho = 0.5$ . The distributions determined from simulation are compared against the theoretical distributions obtained from the general probability given in eq. (16) after integration, i.e.,

$$P(q) = \frac{1}{\mathcal{Z}} \int d\tilde{\Gamma} e^{-\sum_i \left[ \frac{p_i^2}{2m_i} + u_i - Tz_i(u_i, n_i) \right] / (k_B T)} \delta[q - q(\tilde{\Gamma})] \quad (88)$$

where  $q(\tilde{\Gamma})$  is an arbitrary function of the state of the system and  $\mathcal{Z}$  is the normalisation. For the particle internal energy distribution of particle  $i$ , for instance, we have  $q(\tilde{\Gamma}) = u_i$ . No explicit expression can be obtained for the general case, except for the particle momenta<sup>58</sup>, i.e.,

$$P(p_\alpha) \sim e^{-[p_\alpha^2 / (2mk_B T)]} \quad (89)$$

with  $\alpha \equiv (x, y, z)$ . Nevertheless, we can compare the simulated particle probability distributions against theoretical estimates for  $u$ ,  $\theta$  and  $n$  using mean field and saddle point evaluations. For the particle internal energy we have

$$P(u) \sim e^{-[u - Tz(u, \rho)] / (k_B T)} \quad (90)$$

where the system number density  $\rho = N/V$  is used in the theoretical estimate. As evident in Fig. 1, excellent agreement between the simulated and theoretical estimate is found, which further indicates a self-consistent theoretical framework. Along the same lines, the particle temperature distribution is obtained by simply changing the particle internal energy for the particle temperature, with the Jacobian  $\partial u / \partial \theta|_n = C_V$ , i.e.,

$$P(\theta) \sim e^{-[u(\theta) - Tz(\theta, \rho)] / (k_B T)} C_V(\theta, \rho) \quad (91)$$

where for the general model used here,  $C_V$  is a constant. Again, the excellent agreement between the simulated and theoretical distributions indicates the consistency of the methodology proposed here. Finally for the density fluctuations, we have performed Monte Carlo simulations using the equivalent of the Monte Carlo configurational integral<sup>62</sup>, which we will demonstrate elsewhere

$$\langle n \rangle \propto \int d\mathbf{r}_1 \dots d\mathbf{r}_N e^{-\sum_i [Y(n_i) / (k_B T) + \ln \psi(n_i)]} \left( \frac{1}{N} \sum_i n_i \{r_{ij}\} \right) \quad (92)$$

The agreement of the simulated result with the Monte Carlo sampling, the latter based only on the particle internal energy functions, is excellent. We can thus conclude that the model presented is capable of correctly sampling the equilibrium distribution functions, and therefore, its thermodynamic behaviour is consistent.

As further validation of the consistency of the generalised DPDE method, the equivalence of the thermodynamic quantities from isothermal DPD simulations under similar thermodynamic condi-

tions was tested. For the vdW EOS at  $T = 1.5$  and  $\rho = 0.5$ , two different approaches for performing an isothermal DPD simulation were employed. The standard isothermal DPD method was applied, while an alternative approach was implemented by maintaining the particle internal temperatures fixed at the thermostat temperature during a generalised DPDE simulation. In all three approaches, the density-dependent component of the particle interaction potential was still present. Simulated under effectively the same thermodynamic conditions in all three approaches, ensemble averages of the kinetic temperature and the virial pressure were in excellent agreement, where relative to the standard isothermal DPD result, differences of less than 0.1 % were found.

## 5.2 Analysis of the energy conservation

The energy conservation of a MB-FF-EOS within the generalised DPDE framework is considered next. An analysis of the numerical integration scheme presented in Sec. 4.2 is given, however first, a proof that the MB-FF-EOS is a conservative potential is described.

### 5.2.1 Proof that a MB-FF-EOS is a conservative potential

The intent of the proof is to demonstrate that a density- and temperature-dependent many-body force field used within the generalised DPDE framework satisfies a necessary condition of a conservative potential, i.e., the Maxwell relation  $\frac{\partial \mathbf{f}_i}{\partial \mathbf{r}_j} = \frac{\partial \mathbf{f}_j}{\partial \mathbf{r}_i}$ . The proof follows the work of Warren<sup>63</sup> and Moore et al.<sup>31</sup> who considered a many-body force field that has both a distance and density dependence, where they satisfied the necessary requirements relating the corresponding weighting functions. The key distinction of the MB-FF-EOS introduced within the generalised DPDE framework is the temperature dependence, as such, when the force between pairs is determined then,  $\mathbf{f}_{ij}^C = \mathbf{f}_{ij}^C [n_i(\{r_{ij}\}), n_j(\{r_{ij}\}), \theta_i, \theta_j]$ , where  $\theta_i \neq \theta_j$ . The complete proof that a MB-FF-EOS satisfies the Maxwell relation for a conservative potential follows from straightforward, but careful book keeping, and is provided in Supplemental Material B. Satisfying the Maxwell relation ensures that any observed energy drift is due to the numerical integration of the EOM, which is considered in the next section.

As an aside, this proof is valid if a MB-FF-EOS is used in either the original DPDE or generalised DPDE method. However as discussed above, implementing a temperature-dependent particle interaction potential within the DPDE framework requires that the conservative forces are calculated at constant entropy, and not at constant particle internal energy. This allows for the separation of the energy variation due to reversible work from the pure heat transfer in the algorithm. This separation adds the complexity of dealing with the particle temperature and dressed particle temperature simultaneously. In support of these theoretical constructs, from rigorous testing, we have observed that a manifestation of using a MB-FF-EOS within the original DPDE method is energy drift several orders of magnitude higher than the numerical integration error presented below.

### 5.2.2 Analysis of the numerical integration scheme

An analysis of the energy conservation observed for the numerical integration scheme described in Sec. 4.2 is presented next.

Shown in Fig. 2 is the time step size ( $\delta t$ ) dependence of the integration scheme using the LJ MB-FF-EOS for different temperatures at a density of  $\rho = 0.5$ . The energy drift is characterised by a linear fit of the time evolution of the relative total energy,  $[E(t) - E(t = 0)]/E(t = 0)$ , where the slope of this fit is defined as the relative energy drift rate per simulation time ( $t = 5,000$ ). Excellent energy conservation is observed, where not until  $\delta t = 0.05$  does the energy drift become non-negligible, yet still remains small at  $\delta t = 0.1$ .

In Fig. 3, the energy drift rate dependence at different densities and temperatures using  $\delta t = 0.01$  is considered. The isotherms at  $T = 1.5$  and 3 correspond to states in the supercritical phase. The isotherm at  $T = 1$  corresponds to states in the liquid phase, where vapour-liquid phase separation is observed for densities below  $\rho < 0.7$ , and thus are excluded from the figure. For all temperatures, the energy drift increases with density due to the increase in particle pressures determined from the EOS, leading to larger interparticle forces. Moreover, at higher densities, the gradient of the pressure-density behaviour in the EOS results in larger interparticle force fluctuations as the particle density fluctuates. At higher temperature, the energy drift is observed to increase in Figs. 2 and 3, which can also be attributed to larger interparticle forces resulting from the high particle pressures determined from the EOS. Note that the Metropolis procedure developed by Stoltz<sup>64</sup> could be implemented to stabilise the numerical scheme, particularly at smaller values of  $C_V$ .

### 5.2.3 Comparison of the simulated and the thermodynamic behaviour

A comparison of the thermodynamic pressure calculated from the analytical LJ EOS and the virial pressure simulated using the LJ MB-FF-EOS in the generalised DPDE method is presented in Fig. 4. Isotherms are plotted for a range of system densities, where excellent agreement between the thermodynamic and virial pressures are observed. The minor deviations observed at the highest system density  $\rho = 0.8$  stem from the finite spherical cut-off used in the local density, where the dependence on cut-off is considered below. The equivalence of the generalised DPDE virial pressure and the thermodynamic pressure shown in Fig. 4 validates a fundamental thermodynamic consistency between the generalised DPDE method and the macroscopic EOS. An analogous comparison between the thermodynamic pressure calculated from the analytical vdW EOS and the virial pressure from the generalised DPDE simulations is presented in Fig. S1 of the Supplemental Material. Again, excellent agreement between the thermodynamic and virial pressures is observed.

The effect of the spherical cut-off [defined below eq. (3)],  $R_{cut}$ , used in the local density weighting function on the virial pressure is shown in Fig. 5. As expected, with increasing  $R_{cut}$ , the virial pressure converges to the thermodynamic pressure, which follows from the local density converging to the system density with increasing  $R_{cut}$ . The dependence of the virial pressure on  $R_{cut}$  becomes more pronounced with increasing system density, which again is based on the approximation of the local density relative to the system density, i.e., related to the suppression of the density fluctuations. The dependence of  $R_{cut}$  on the energy conservation

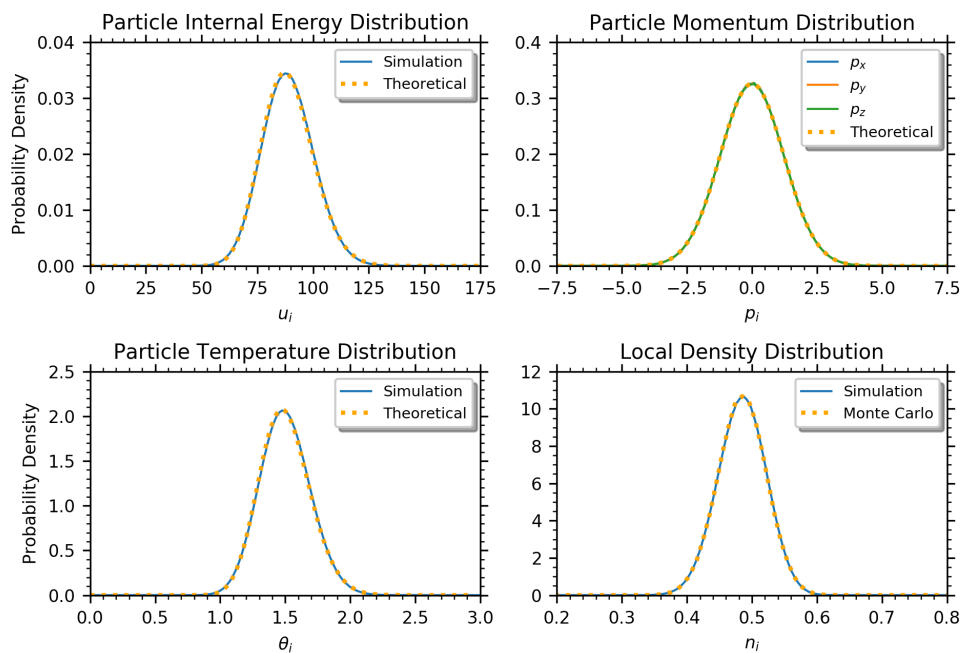


**Fig. 1** Equilibrium probability distributions for the vdW MB-FF-EOS at  $T = 1.5$  and  $\rho = 0.5$ : (top left) particle internal energy; (bottom left) particle temperature; (top right) particle momentum; (bottom right) local density. Dashed lines are the probability distributions given in eqs. (90), (91), (89), and (92), respectively, while solid lines are determined from a generalised DPDE simulation. Due to each of the particle momenta being nearly identical, the plots for each component are indistinguishable.

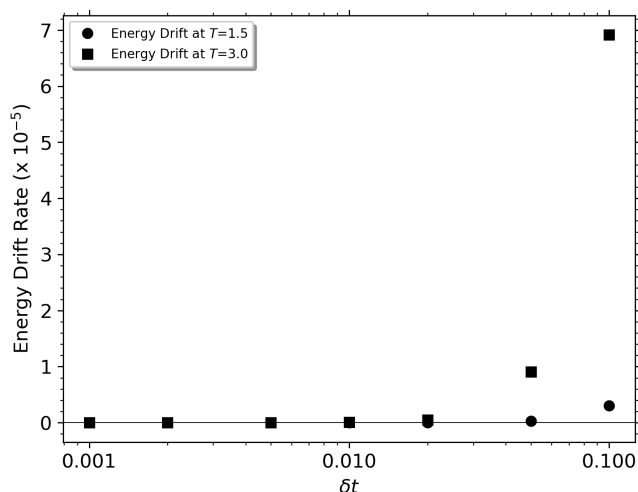


**Fig. 2** Total energy drift rate dependence on time step size,  $\delta t$ , for the numerical integration scheme of the generalised DPDE method presented in Sec. 4.2. Data is presented for the LJ MB-FF-EOS at  $\rho = 0.5$  and  $T = 1.5$  (circles), and  $T = 3$  (squares) on the semi-log plot.

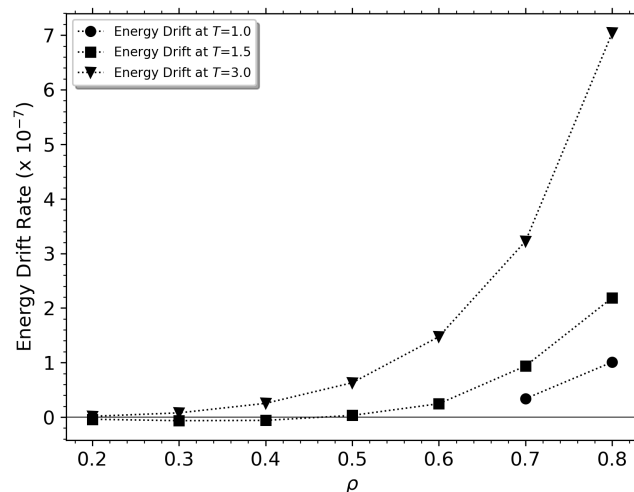


**Fig. 3** Effect of system density  $\rho$  on the total energy drift rate for the LJ MB-FF-EOS at  $T = 1$  (circles),  $T = 1.5$  (squares), and  $T = 3$  (triangles) using  $\delta t = 0.01$ . Dotted lines are provided for visual clarity only.

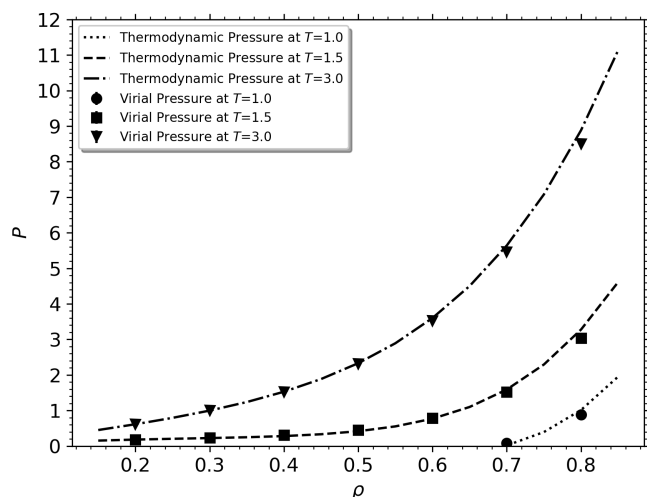


**Fig. 4** Comparison of the thermodynamic pressure calculated from the analytical LJ EOS (lines) and the virial pressure simulated using the LJ MB-FF-EOS in the generalised DPDE method (symbols) at  $T = 1$  (circles),  $T = 1.5$  (squares), and  $T = 3$  (triangles). Standard deviations calculated from the generalised DPDE simulations are smaller than the plotted data points.

was also analysed, and although not shown here, the total energy drift was found to increase as  $R_{cut}$  decreases. This is due to particles entering/exiting the spherical cut-off over a time step, where for smaller  $R_{cut}$ , this results in a larger change in local density, and thus a larger change in the magnitude of the force over the time step.

A parametric study of the dependence of the heat capacity used in the DPDE particle EOS,  $C_V$ , the momentum coefficient  $\gamma$ , and the heat coefficient  $\kappa$  on the steady-state particle probability distributions was performed using the generalised DPDE method. Fig. 6 demonstrates the dependence of the heat capacity on the particle temperature distribution. Not shown here, but as expected, the local density and particle momentum distributions do not exhibit a dependence on the value of  $C_V$ . Similarly, as expected, no dependence of the steady-state particle probability distributions was exhibited for the various choices of  $\gamma$  and  $\kappa$ . The complete set of particle probability distributions for this parametric study is given in Supplemental Material C, D, and E.

### 5.3 Non-equilibrium simulations

As a further test of both the generalised DPDE method and the numerical integration stability, two different non-equilibrium simulation scenarios were considered. First, an adiabatic flash heating simulation was performed, which is a common initiation scenario for simulating the thermal response of material models. Then, fluid phase separation was demonstrated, which is a key phenomenon when simulating complex fluids of practical interest. Both simulation scenarios provide a means of assessing the non-equilibrium behaviour of the method, where thermodynamic variables are monitored as the system evolves to an equilibrated state while maintaining constant energy conditions.

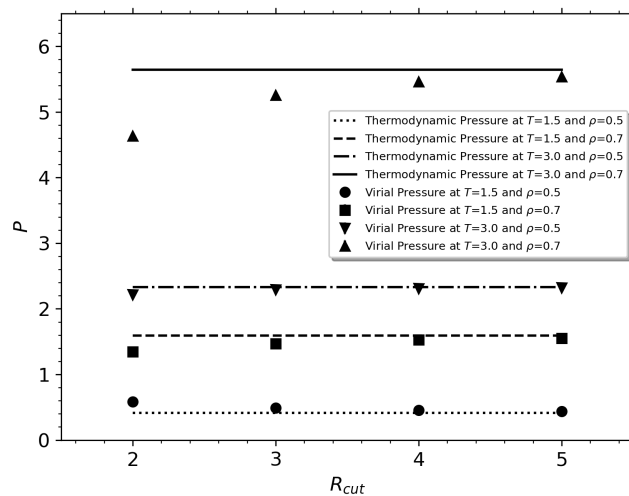


**Fig. 5** Effect of the spherical cut-off,  $R_{cut}$ , used in the local density weighting function on the simulated virial pressure for the LJ MB-FF-EOS in the generalised DPDE method (symbols) at the  $T$  and  $\rho$  shown in the legend. The thermodynamic pressure calculated from the analytical LJ EOS at these state points is also shown (lines). Standard deviations calculated from the generalised DPDE simulations are smaller than the plotted data points.

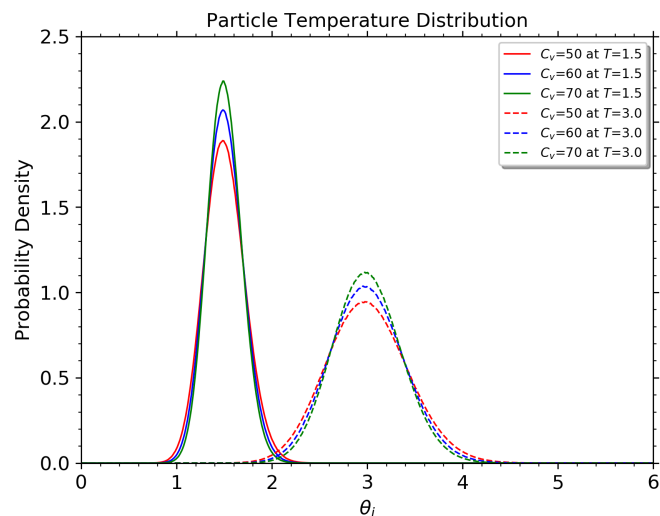


**Fig. 6** Effect of the heat capacity,  $C_V$ , used in the DPDE particle EOS on the particle temperature distribution,  $\theta_i$ .  $\rho = 0.5$  for all cases shown.

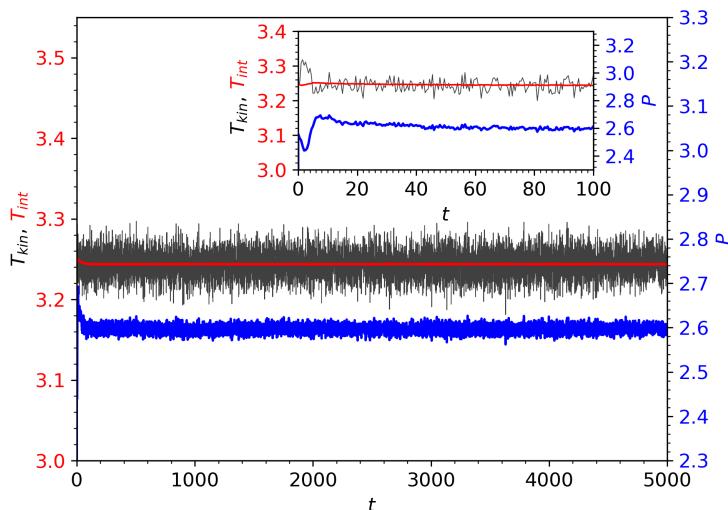


**Fig. 7** Slab-heating response shown as the time evolution of the kinetic temperature  $T_{kin}$  (black), internal temperature  $T_{int}$  (red), and the virial pressure  $P$  (blue) for a generalised DPDE simulation using the LJ MB-FE-EOS at  $\rho = 0.5$ . A box-centred slab of particles comprising 50 % of all particles in the box was instantaneously heated by  $T_{heat} = 5$  at  $t = 0$ .

### 5.3.1 Flash heating response

Adiabatic flash heating simulations were performed by instantaneously heating a slab of particles to a target temperature of  $T_{heat} = 5$ . Initially, the system was equilibrated at  $T = 1.5$  and  $\rho = 0.5$  for 5,000 time steps (using  $\delta t = 0.01$ ). After equilibration, a box-centred slab of particles consisting of half of the total number of particles was instantaneously heated via both a rescaling of the particle velocities and a resetting of the particle temperatures to  $T_{heat}$ . The adiabatic flash heating simulations were conducted for an additional 5,000 time steps, ensuring that steady-state behaviour was achieved. Temporal data of the system thermodynamic properties were collected every 50 time steps.

Shown in Fig. 7 are the time evolution of the kinetic temperature  $T_{kin} = \sum_i (p_i^2/m_i)/(3N-3)$ , internal temperature  $T_{int} = \sum_i \theta_i/N$ , and the virial pressure  $P$ , where a total energy drift of  $10^{-7}$  was observed. The inset of Fig. 7 displays the early time behaviour, where the initial abrupt changes in  $T_{kin}$  and  $P$  are due to the relaxation of the artificially-created heated slab interface. Nonetheless, it is evident that  $T_{kin}$  and  $T_{int}$  quickly equalised, where at steady state, the ensemble averages of  $\langle T_{kin} \rangle$  and  $\langle T_{int} \rangle$  are in excellent agreement (average relative difference of less than 0.01%), indicative of numerical stability and self-consistency within the simulation.

### 5.3.2 Vapour-liquid phase separation simulations

A demonstration of spontaneous phase separation using the generalised DPDE method was performed. For the LJ EOS, a state point within the vapour-liquid coexistence region was chosen,  $T = 1$  and  $\rho = 0.2$ , where the initial configuration was a simple cubic lattice structure of size  $68.4 \times 38.5 \times 51.3$  length units. Other computational details for this simulation are:  $\delta t = 0.01$ ;  $C_V = 60$ ;  $R_{cut} = 4$ ;  $\gamma = 4.5$ ; and  $\kappa = 1$ . Shown in Fig. 8 are the

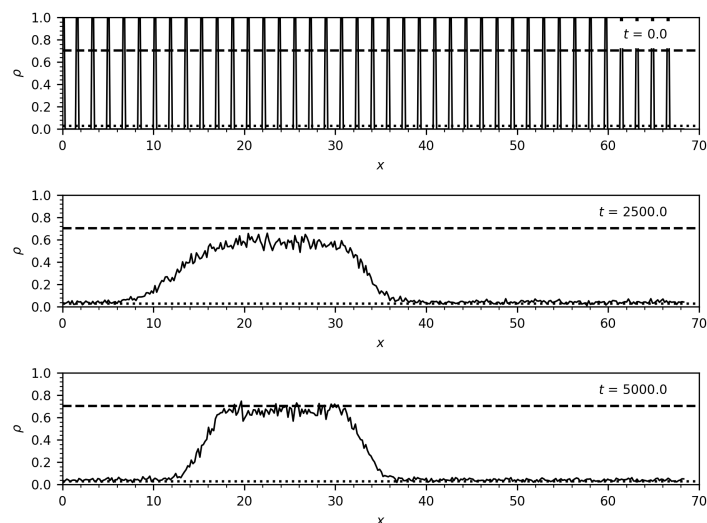


**Fig. 8** Number density profiles determined from slabs along the  $x$ -direction from a generalised DPDE simulation at various times as vapour-liquid phase separation occurs for the LJ fluid. The initial configuration was a simple cubic lattice structure at  $T = 1$  and  $\rho = 0.2$ . The vapour and liquid coexistence densities determined elsewhere<sup>65</sup> are shown as dotted and dashed lines, respectively.

number density profiles along the  $x$ -direction at various times. At  $t = 0$ , the cubic lattice structure is clearly evident, while as phase separation spontaneously occurs, the number density profiles indicate condensation occurring in the form of a slab of particles. For comparison, the vapour and liquid coexistence densities determined using the LJ two-body hard-core interaction potential<sup>65</sup> are shown. The slight under-prediction of these coexisting densities is attributed to the local density approximation, which under-estimates the system density. Fig. 9 presents the time evolution of the kinetic temperature  $T_{kin}$ , internal temperature  $T_{int}$ , and the virial pressure  $P$  as the phase separation occurs. The saturation pressure determined elsewhere<sup>65</sup> is shown, where again the slight discrepancy with the generalised DPDE simulation result is attributed to the local density approximation. A configurational snapshot of the vapour-liquid coexistence at equilibrium is provided in Fig. S2 of the Supplemental Material. A surface tension of  $\sigma = 0.18$  was estimated from the ensemble averages of the pressure tensor components, as described elsewhere<sup>66</sup>.

A practical computational detail regarding the local density when simulating the vapour phase is discussed here. The local density calculation does not include the self-particle, which could be numerically problematic if no particles are within the spherical radius, since  $n_i = 0$  precisely. For a large  $R_{cut}$ , this is less likely to occur even in the vapour phase. And while this did not occur for the simulation considered here, nevertheless, a practical solution is worth mentioning. In the occurrence when no particles are found within the spherical radius,  $n_i$  could be set to a small, but non-zero value, while setting the particle pressure  $\pi_i = 0$ . In this case, the interparticle forces for particle  $i$  will be zero, yet still numerically defined.

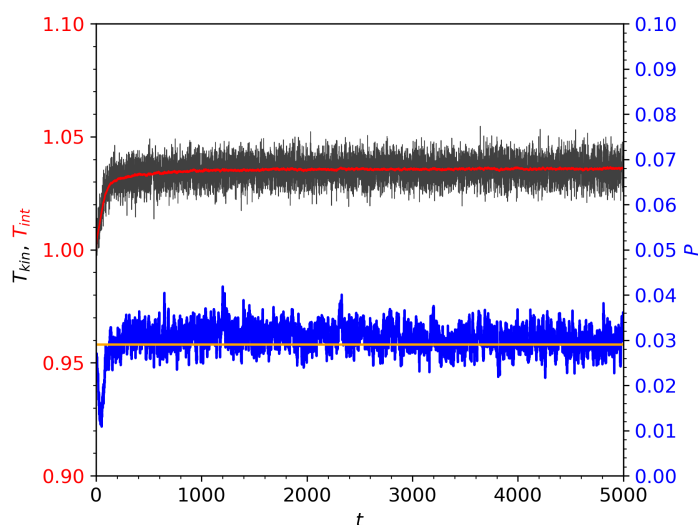


**Fig. 9** The time evolution of the kinetic temperature  $T_{kin}$  (black), internal temperature  $T_{int}$  (red), and the virial pressure  $P$  (blue) for the same vapour-liquid phase separation shown in Fig. 8. The saturation pressure of  $0.029(\pm 0.022)$  determined elsewhere<sup>65</sup> is shown as the orange line.

## 6 Conclusions

A generalised, energy-conserving dissipative particle dynamics method appropriate for the non-isothermal simulation of particle interaction force fields that are both density- and temperature-dependent was presented. A detailed derivation of the EOM was formulated in a bottom-up manner, preserving a direct link to the higher resolution scale. Practical considerations for implementing the generalised DPDE method were given, along with demonstrations using analytical equation-of-states for the van der Waals and Lennard-Jones fluids, which were used to validate the algorithm and the thermodynamic consistency of the method. From the analysis presented here, it can be inferred that a fundamental inconsistency exists if the original DPDE method is straightforwardly used to simulate a temperature-dependent force field. Effectively, when the particle temperature is used in both the MB-FF-EOS and the DPDE particle EOS, a thermodynamically rigorous link between these two quantities is lacking, if applied in the original DPDE method. As such, it is not guaranteed that with the original DPDE EOM the appropriate thermodynamic consistency will be satisfied when a temperature-dependent force field is implemented, which manifests in a lack of energy conservation during the simulation. With the growing emphasis on bottom-up CG models that depend on both the density and temperature, the generalised DPDE method will be a key method for simulating these CG models in non-isothermal conditions.

While the final expressions for the EOM have similarities to those of the energy form of the SDPD method<sup>40</sup>, the formulation of the EOM for each method are distinctively different. In the SDPD method, the formulation begins by considering collections of molecules effectively as fields, and subsequently translating these fields into particles following a procedure that is not unequivocal<sup>67</sup>. The fluctuations are introduced within the spirit of fluctuating hydrodynamics, namely, as small perturbations of

the macroscopic fields. In contrast, for the generalised DPDE method, each particle is considered to be embedded in a local volume and embodying thermodynamic properties, due to the coarsened degrees-of-freedom. Compared with isothermal DPD, the finiteness of the particle heat capacity produces particle internal energy fluctuations that entangle with the dynamics of the fields, which affects the thermodynamic averages in a non-trivial way, as we have shown in this article. Thus, for the generalised DPDE method, a fundamental link is maintained with the underlying physical system at the higher resolution scale. In contrast with the top-down formulations such as SDPD, the bottom-up approaches allow for a clear and consistent formulation of the fundamental physical principles affecting the dynamics, as well as the thermodynamic properties of the macroscopic physical system, as acknowledged in the literature<sup>67,68</sup>. We thus believe that the proposed generalised DPDE method is a step forward in the construction of mesoscopic models from the coarse-graining of molecularly-defined systems.

Although the demonstrations were performed using an analytical EOS, the generalised DPDE method is not limited to such models. Rather, density- and temperature-dependent models developed from higher resolution models are also suitable, such as those determined using bottom-up coarse-graining approaches that have been rapidly developed in recent years<sup>16,69–73</sup>, which include the effect of the non-Markovian response<sup>73–75</sup>, and the development of a conceptual framework for the operation of coarse-graining<sup>76–79</sup>.

MB-FF-EOS models have many attributes as CG models, including robust transferability and scaling invariance, while overcoming unphysical ordered phase behaviour that often afflicts CG models<sup>17</sup>. Moreover, appropriate CG mapping of a set of non-bonded atoms or molecules “moving coherently”, may be best realised by a MB-FF-EOS<sup>27</sup>. Applications of the generalised DPDE method using other MB-FF-EOS such as the Exponential-6 EOS recently used for fluid mixtures at extreme pressures and temperatures<sup>17</sup> are underway in our group. Similarly, our current dissipative particle dynamics with reactions framework<sup>5</sup> will be adapted for the generalised DPDE method, which entails simultaneously simulating a CG model that is density- and temperature-dependent along with a CG model that is density-dependent only.

Finally, the derivation of the macroscopic thermodynamic properties as well as the transport coefficients from the different models of current interest discussed here were not addressed in this manuscript, but have been left for future work by our group. Also beyond the scope of the present work is a study of the dependence of the level of coarsening on the thermodynamic and transport properties<sup>80</sup>.

## Conflicts of interest

There are no conflicts to declare.

## Acknowledgements

The authors are grateful to Gabriel Stoltz (École des Ponts ParisTech) for insightful discussions regarding this work. ML acknowledges funding from the ERDF/ESF project “UniQSurf-Centre of biointerfaces and hybrid functional materials”

(No. CZ.02.1.01/0.0/0.0/17\_048/0007411), and from the Internal Grant Agency of J. E. Purkinje University (project No. UJEP-SGS-2019-53-005-3). JKB and JPL acknowledge support in part by the Office of Naval Research (BAA number 12-001). This work was supported in part by a grant of computer time from the DoD High Performance Computing Modernization Program at the ARL, Navy, AFRL and ERDC Supercomputing Resource Centers. JBA and ADM wish to thank the Ministerio de Ciencia, Innovación y Universidades (MCIU), of the Spanish Government for financial support, grant CTQ2017-84998-P “Segregación molecular a múltiples escalas en sistemas no tensioactivos para la obtención de materiales avanzados”.

## A More complex molecular models

Here the reader can find the functional forms of more general mesoscopic MB-FF-EOS models. In particular, we introduce the general functional form for systems with particle pressures that depend linearly on the particle temperature  $\theta$ , and with an arbitrary dependence on the local density  $n$ . Further, we present the analytical expressions of the LJ fluid EOS, as described in ref.<sup>59</sup>.

### A.1 General form for systems with linear dependence on the particle temperature

Analogous to the vdW EOS given in eq. (29), let us assume a system in which the pressure may be density dependent, but its particle temperature dependence is linear. Within these conditions, the general form of the mesoscopic MB-FF-EOS depends upon two functions of  $n$ ,  $\psi(n)$  and  $\mathcal{V}(n)$ , and can be written as

$$u(s, n) = C_V \theta_0 e^{s/C_V} \psi(n)^{k_B/C_V} + \mathcal{V}(n) \quad (93)$$

The general equation for the particle pressure takes the form

$$\begin{aligned} \pi &= n^2 \left. \frac{\partial f}{\partial n} \right|_{\theta} \\ &= k_B \theta \frac{n^2 \psi'(n)}{\psi(n)} + n^2 \mathcal{V}'(n) \end{aligned} \quad (94)$$

The particle entropy function is then

$$s(u, n) = C_V \ln \left[ \frac{u - \mathcal{V}(n)}{C_V \theta_0} \right] - k_B \ln \psi(n) \quad (95)$$

while the dressed particle entropy is given by

$$z(u, n) = (C_V - k_B) \ln \left[ \frac{u - \mathcal{V}(n)}{C_V \theta_0} \right] - k_B \ln \psi(n) \quad (96)$$

Some special cases are analysed below.

#### A.1.1 DPDE with many-body, temperature-independent EOS

Let us consider the classical DPDE model<sup>20</sup> extended to density-dependent potential forces<sup>17,31,34,35</sup>, i.e.,

$$\frac{\pi}{n^2} = \mathcal{V}'(n) \quad (97)$$

Hence,

$$u(s, n) = C_V \theta_0 e^{s/C_V} + \mathcal{V}(n) \quad (98)$$

From this expression we arrive at the particle entropy function

$$s(u, n) = C_V \ln \left[ \frac{u - \mathcal{V}(n)}{C_V \theta_0} \right] \quad (99)$$

Setting  $\mathcal{V}(n) = 0$ , one recovers the ideal gas with energy conservation.

### A.2 Mesoscopic ideal gas MB-FF-EOS

The simplest model that can be addressed within this formalism is based on the response of the particles following an ideal gas MB-FF-EOS, i.e.,

$$\pi = k_B \theta n \quad (100)$$

In this case, assuming again that the heat capacity  $C_V$  is constant, we can write

$$u(s, n) = C_V \theta_0 e^{s/C_V} n^{k_B/C_V} \quad (101)$$

The particle entropy function is then

$$s(u, n) = -k_B \ln n + C_V \ln \left( \frac{u}{C_V \theta_0} \right) \quad (102)$$

This MB-FF-EOS provides the commonly used factor in the force definition of the SPH method, namely

$$\frac{\pi}{\pi_0} = \left( \frac{n}{n_0} \right)^{k_B/C_V} \quad (103)$$

The model parameter  $\gamma$  in SPH would then be identified here as  $k_B/C_V$ .

### A.3 Mesoscopic LJ MB-FF-EOS

An analytical EOS for systems with LJ interactions has been derived from extensive simulations of these systems in terms of molecular parameters<sup>59</sup>. A summary of this analytical EOS is given here. Let us assume that the underlying physical system is defined in terms of the packing fraction

$$\eta = \frac{\pi}{6} n d_{\text{hBH}}^3 \quad (104)$$

where  $d_{\text{hBH}}$  is the particle diameter

$$d_{\text{hBH}} = \int_0^{R_m} \left[ 1 - e^{-u_0(r)/(k_B \theta)} \right] dr \quad (105)$$

If  $u_{\text{LJ}}(r)$  is the LJ potential

$$u_{\text{LJ}}(r) = 4\epsilon_{\text{LJ}} \left[ \left( \frac{\sigma_{\text{LJ}}}{r} \right)^{12} - \left( \frac{\sigma_{\text{LJ}}}{r} \right)^6 \right]$$

then  $u_0(r) \equiv u_{\text{LJ}}(r) - u_{\text{LJ}}(R_m)$  and  $R_m = 2^{1/6} \sigma_{\text{LJ}}$  is the position of the minimum of the LJ potential. The hard sphere contribution to the particle Helmholtz free energy is given by

$$f_{\text{HS}} = k_B \theta \left[ \frac{5}{3} \ln(1 - \eta) + \frac{\eta(34 - 33\eta + 4\eta^2)}{6(1 - \eta)^2} \right] \quad (106)$$

The final expression for the particle Helmholtz free energy is

$$f = f_{\text{HS}} + n k_B \theta e^{-\gamma m^2 \Delta B_{2,\text{hBH}}(k_B \theta)} + \sum_{ij} C_{ij} \theta^{i/2} n^j \quad (107)$$

where the residual second virial coefficient is defined as  $\Delta B_{2,\text{hBH}} = B_{2,\text{LJ}} - \frac{2\pi}{3} d_{\text{hBH}}^3$  with

$$B_{2,\text{LJ}} = -\frac{1}{2} \int \left[ 1 - e^{-u_{\text{LJ}}(r)/(k_B\theta)} \right] d\mathbf{r} \quad (108)$$

being the second virial coefficient of a LJ system.  $B_{2,\text{LJ}}$  is given in closed form as

$$B_{2,\text{LJ}} = \frac{2\pi}{3} \sigma_{\text{LJ}}^3 \sqrt{2\pi} \left( \frac{\epsilon_{\text{LJ}}}{k_B\theta} \right)^{1/4} H_{\frac{1}{2}} \left( -\sqrt{\frac{\epsilon_{\text{LJ}}}{k_B\theta}} \right)$$

where  $H_{1/2}$  represents the Hermite function of order 1/2. The constants  $C_{ij}$  are given in ref.<sup>59</sup>.

## B Derivation of the statistical properties of the random terms

In this appendix, we give a detailed derivation of the statistical properties of the random terms appearing in the stochastic equations of motion, eq. (75) and eq. (80). Our derivation does not follow the traditional formulation through the corresponding Fokker-Planck equation<sup>20</sup>, but instead we calculate the first and second moment of the probability distribution, either using eq. (12) or eq. (16), depending on the independent variables coming into play. This perspective allows us to have a more mechanistic view on the processes, as we will use the discrete form of the algorithms, instead of stochastic differential equations, the latter entangled with Itô-Stratonovich kind of dilemmas. The algorithm formulation in a discrete form is well defined. Our choice in eqs. (74) and (78) corresponds to a causal representation of the dynamics.

Furthermore, the calculation of the moments of the distribution is based on the detailed balance principle satisfied by physical systems in thermodynamic equilibrium<sup>57</sup>. Schematically, the algorithm provides a transition from a space state point  $\Gamma = (\{\mathbf{p}_i\}, \{\mathbf{r}_i\}, \{u_i\})$  at  $t$  into a new point  $\Gamma'$  at  $t + \delta t$ . The new point is a function of the original one, the dynamic properties of the system, and of the random numbers  $\Omega$ . The overall algorithm can be written in the following general form

$$\Gamma' = \Gamma_d[\Gamma, \Omega; \delta t] \quad (109)$$

where  $\Gamma_d$  represents the generic function that provides the dynamics. Its arguments represent the variables of which this function depends. The transition probability is thus given by

$$w(\Gamma \rightarrow \Gamma') \delta t = \langle \delta(\Gamma' - \Gamma_d[\Gamma, \Omega]) \rangle_{\Omega} \quad (110)$$

The subscript  $\Omega$  indicates that the average has to be determined over all the realisations of the random force. From this expression, due to the causal nature of the algorithm, it follows that

$$\int d\Gamma' w(\Gamma \rightarrow \Gamma') \delta t = \int d\Gamma' \langle \delta(\Gamma' - \Gamma_d[\Gamma, \Omega]) \rangle_{\Omega} = 1 \quad (111)$$

The reverse trajectory is defined as  $\Gamma^* \rightarrow \Gamma^{*'}$  where  $\Gamma^* \equiv (\{-\mathbf{p}_i'\}, \{\mathbf{r}_i'\}, \{u_i'\})$  and  $\Gamma^{*'} \equiv (\{-\mathbf{p}_i\}, \{\mathbf{r}_i\}, \{u_i\})$ . The change of sign depends on the parity under time reversal of the variable<sup>57</sup>.

Thus, detailed balance indicates that<sup>81</sup>

$$P_{\text{eq}}(\Gamma) w(\Gamma \rightarrow \Gamma') = P_{\text{eq}}(\Gamma^*) w(\Gamma^* \rightarrow \Gamma^{*'}) \quad (112)$$

The stochastic process described by the algorithm satisfies a master equation with the transition probabilities given by eq. (110). The calculation of the Fokker-Planck approximation to the master equation requires the evaluation of the first and second moments of the distribution of the variable transitions<sup>57</sup>. This last equation permits us to calculate the moments of the distribution. If we restrain the analysis up to second order moments, we are under the same degree of approximation as the Fokker-Planck equation itself.

### B.1 Momentum equation

To obtain the first moment of the momentum distribution, we evaluate

$$\begin{aligned} \int d\Gamma d\Gamma' P_{\text{eq}}(\Gamma) \mathbf{p}_i' w(\Gamma \rightarrow \Gamma') &= \int d\Gamma d\Gamma' P_{\text{eq}}(\Gamma^*) \mathbf{p}_i' w(\Gamma^* \rightarrow \Gamma^{*'}) \\ &= - \int d\Gamma^* d\Gamma^{*'} P_{\text{eq}}(\Gamma^*) \mathbf{p}_i' w(\Gamma^* \rightarrow \Gamma^{*'}) \\ &= - \int d\Gamma^* P_{\text{eq}}(\Gamma^*) \mathbf{p}_i^* \\ &= \langle \mathbf{r}_i \rangle \end{aligned} \quad (113)$$

Using the equation of motion (73), together with eq. (110), on the left-hand-side of this last equation, one obtains

$$\int d\Gamma P_{\text{eq}}(\Gamma) \left( \mathbf{p}_i + \sum_{j \neq i} \mathbf{f}_{ij}^C \delta t + \sum_{j \neq i} \mathbf{f}_{ij}^D \delta t + \sum_{j \neq i} \langle \delta \mathbf{p}_{ij}^R \rangle_{\xi} \right) = 0 \quad (114)$$

As  $\mathbf{p}_i$  as well as  $\sum_{j \neq i} \mathbf{f}_{ij}^D$ , cf. eq. (65), are even functions of momenta, their equilibrium value is zero. Also, in view of eq. (75),  $\langle \delta \mathbf{p}_{ij}^R \rangle_{\Omega} = 0$ . Finally, the equilibrium average of the conservative force requires some more algebra. First, the integration with respect to the momenta and entropies factorises, and can be readily performed, leaving only an integration over the particle positions. As the system is invariant under the variation of the centre of mass  $\mathbf{R}$ , we introduce  $\int d\mathbf{R} \delta(\mathbf{R} - 1/N \sum_i \mathbf{r}_i) = 1$ , and integrate with respect to  $\mathbf{r}_i$  to get

$$\int d\Gamma P_{\text{eq}}(\Gamma) \sum_{j \neq i} \mathbf{f}_{ij}^C = N \int d\mathbf{R} \int d\mathbf{r}_1 \dots d\mathbf{r}_N P(\tilde{\mathbf{x}}) \frac{1}{N} \sum_{j \neq i} \frac{\partial U(\tilde{\mathbf{x}})}{\partial \mathbf{r}_j} \Big|_{s_i}$$

where  $U \equiv \sum_i u_i$ . We have also used the fact that due to the translational invariance,  $\partial U / \partial \mathbf{r}_i = -\sum_{j \neq i} \partial U / \partial \mathbf{r}_j$ . In this equation we have written  $\tilde{\mathbf{x}} = (\mathbf{r}_1, \mathbf{r}_2, \dots, [N\mathbf{R} - \sum_{j \neq i} \mathbf{r}_j], \dots, \mathbf{r}_N)$ , where the expression between brackets replaces the vector  $\mathbf{r}_i$ . Notice the overall factor  $N$  that appears from the integration of the  $\delta$ -function with respect to  $\mathbf{r}_i$ . The factor  $1/N$  has been explicitly introduced because of an important point that we demonstrate in the follow-

ing. Let us calculate the derivative in this last equation

$$\begin{aligned} \frac{\partial}{\partial \mathbf{r}_j} U(\bar{\mathbf{x}}) &= \frac{\partial}{\partial \mathbf{r}_j} \sum_k u_k(\bar{\mathbf{x}}) \\ &= \sum_{k \neq j} \left( \frac{\partial u_j}{\partial n_j} \mathbf{w}_{jk} - \frac{\partial u_k}{\partial n_k} \mathbf{w}_{kj} \right)_{s_j} - \sum_{k \neq i} \left( \frac{\partial u_i}{\partial n_i} \mathbf{w}_{ik} - \frac{\partial u_k}{\partial n_k} \mathbf{w}_{ki} \right)_{s_i} \\ &= -\mathbf{f}_j^C + \mathbf{f}_i^C \end{aligned} \quad (115)$$

where we have defined  $\mathbf{w}_{jk} \equiv \mathbf{e}_{ij} w' / [w]$  for the ease of notation. The second term appears due to the constrained integration of the  $i^{\text{th}}$  coordinate in  $\bar{\mathbf{x}}$ . The summation over  $j$  then yields

$$\sum_{j \neq i} \frac{\partial}{\partial \mathbf{r}_j} \sum_k u_k(\bar{\mathbf{x}}) = -\sum_{j \neq i} \mathbf{f}_j^C + (N-1)\mathbf{f}_i^C = N\mathbf{f}_i^C$$

where  $\sum_j \mathbf{f}_j^C = 0$  has been used. Hence, we can write

$$\begin{aligned} \int d\Gamma P_{\text{eq}}(\Gamma) \sum_{j \neq i} \mathbf{f}_j^C &= -Nk_B T \int d\mathbf{R} \int d\mathbf{r}_N \cdot \left( \frac{1}{N} \sum_{j \neq i} \frac{\partial}{\partial \mathbf{r}_j} P(\bar{\mathbf{x}}) \right)_{s_i} \\ &= 0 \end{aligned} \quad (116)$$

Partial integration has been used to give the last equality.

The calculation of the first moment simply demonstrates the consistency of the algorithm. If the left-hand-side of eq. (113) were not zero, it would indicate that extra terms, often misleadingly called *spurious drift*, should be added.

More interesting is the evaluation of the second moment of the momenta. Similarly as in eq. (113), we aim at calculating here

$$\begin{aligned} \int d\Gamma d\Gamma' P_{\text{eq}}(\Gamma) \mathbf{p}_i' \mathbf{p}_j' w(\Gamma \rightarrow \Gamma') &= \int d\Gamma d\Gamma' P_{\text{eq}}(\Gamma^*) \mathbf{p}_i' \mathbf{p}_j' w(\Gamma^* \rightarrow \Gamma'^*) \\ &= \int d\Gamma^* d\Gamma'^* P_{\text{eq}}(\Gamma^*) \mathbf{p}_i^* \mathbf{p}_j^* w(\Gamma^* \rightarrow \Gamma'^*) \\ &= \int d\Gamma^* P_{\text{eq}}(\Gamma^*) \mathbf{p}_i^* \mathbf{p}_j^* \\ &= \langle \mathbf{p}_i \mathbf{p}_j \rangle \end{aligned} \quad (117)$$

for  $j \neq i$ . Integrating the left-hand-side of this equation with respect to  $\Gamma'$  and using eq. (110), one can write

$$\begin{aligned} \int d\Gamma P_{\text{eq}}(\Gamma) \left[ \mathbf{p}_i \sum_k \boldsymbol{\gamma}_{jk} \cdot \frac{\mathbf{p}_k}{m} \delta t + \mathbf{p}_j \sum_l \boldsymbol{\gamma}_{il} \cdot \frac{\mathbf{p}_l}{m} \delta t \right. \\ \left. + \sum_{k \neq i, l \neq j} \langle \delta \mathbf{p}_{ik}^R \delta \mathbf{p}_{jl}^R \rangle_{\xi} \right] = 0 \end{aligned} \quad (118)$$

where only terms up to  $\mathcal{O}(\delta t)$  have been retained. Moreover, terms linear in  $\delta \mathbf{p}^R$  vanish because the random force is not correlated with variables at the same time, due to the implicit causal hypothesis. The terms concerning the conservative force also vanish due to the fact that the average over momenta and average over positions can be independently performed, and in the calculation of the first moment we have seen that both van-

ish. Here for compactness, we have introduced the shorthand notation  $\boldsymbol{\gamma}_{ij} = \gamma_{ij} \mathbf{e}_{ij} \mathbf{e}_{ij}$ , together with the definition of the self-coefficient  $\boldsymbol{\gamma}_{ii} \equiv -\sum_{j \neq i} \boldsymbol{\gamma}_{ij}$ . We then proceed to the calculation of the average of the quadratic terms in the momenta with respect to the momenta distributions, i.e.,

$$\int d\mathbf{p}_1 \dots d\mathbf{p}_N e^{-\sum_l p_l^2 / (2m_l k_B T)} \delta \left( \sum_l \mathbf{p}_l \right) \frac{\mathbf{p}_i}{m} \boldsymbol{\gamma}_{jk} \cdot \frac{\mathbf{p}_k}{m} \quad (119)$$

where we have introduced the constraint that the total momentum is conserved, which we have chosen to be zero without loss of generality. Let us initially consider explicitly the case  $j \neq i$ . Integrating with respect to  $\mathbf{p}_j$ , the previous expression is equal to

$$-k_B T \int d\mathbf{p}_1 \dots d\mathbf{p}_N \frac{\mathbf{p}_i}{m} \boldsymbol{\gamma}_{jk} \cdot \frac{\partial}{\partial \mathbf{p}_k} e^{-\sum_{l \neq j} p_l^2 / (2m_l k_B T)} e^{-(\sum_{l \neq j} p_l)^2 / (2m_l k_B T)} \quad (120)$$

Partial integration and the fact that the remaining momenta (all but  $\mathbf{p}_j$ , which is not present in the argument) are independent, permits us to write that this last expression is equal to

$$\frac{k_B T}{m} \boldsymbol{\gamma}_{jk} \delta_{ik} \quad (k \neq i)$$

The term  $i = j$  follows by writing  $\mathbf{p}_j = -\sum_{l \neq j} \mathbf{p}_l$  in eq. (120) and repeating the evaluation. Hence, the average in eq. (119) has the form

$$\begin{aligned} \int d\mathbf{p}_1 \dots d\mathbf{p}_N e^{-\sum_l p_l^2 / (2m_l k_B T)} \delta \left( \sum_l \mathbf{p}_l \right) \frac{\mathbf{p}_i}{m} \boldsymbol{\gamma}_{jk} \cdot \frac{\mathbf{p}_k}{m} \\ = \frac{k_B T}{m} \boldsymbol{\gamma}_{jk} [\delta_{ik}(1 - \delta_{ij}) - \delta_{ij}] \end{aligned}$$

Further, we can write, from eq. (118)

$$\begin{aligned} \int d\Gamma P_{\text{eq}}(\Gamma) \left\{ 2 \frac{k_B T}{m} \left[ \boldsymbol{\gamma}_{ij}(1 - \delta_{ij}) - \delta_{ij} \sum_k \boldsymbol{\gamma}_{ik} \right] \delta t \right. \\ \left. + \sum_{k \neq i, l \neq j} \langle \delta \mathbf{p}_{ik}^R \delta \mathbf{p}_{jl}^R \rangle_{\xi} \right\} = 0 \end{aligned} \quad (121)$$

where the symmetry of the friction matrices  $\boldsymbol{\gamma}_{ij} = \boldsymbol{\gamma}_{ji}$  has been used. On the other hand, the random momenta satisfy

$$\begin{aligned} \sum_{k \neq i, l \neq j} \langle \delta \mathbf{p}_{ik}^R \delta \mathbf{p}_{jl}^R \rangle_{\xi} &= \sum_{k \neq i, l \neq j} \sigma_{ik} \sigma_{jl} \langle \xi_{ik} \xi_{jl} \rangle \mathbf{e}_{ik} \mathbf{e}_{jl} \delta t \\ &= \left[ \sum_{k \neq i} \sigma_{ik}^2 \delta_{ij} \mathbf{e}_{ik} \mathbf{e}_{ik} - \sigma_{ij}^2 (1 - \delta_{ij}) \mathbf{e}_{ij} \mathbf{e}_{ij} \right] \delta t \end{aligned} \quad (122)$$

The choice

$$\sigma_{ij} = \sqrt{k_B (\theta_i + \theta_j) \gamma_{ij}} \quad (123)$$

identically satisfies eq. (121), and therefore is the appropriate fluctuation-dissipation theorem. Notice that as the equilibrium average in the first term in eq. (121) is proportional to  $T$ , the fluctuation-dissipation theorem should be proportional to the proper particle temperature estimator, namely  $\theta$ .

## B.2 Energy equation

To begin, we calculate the first moment of the energy distribution using eq. (112). Analogously as in the previous case, we can write

$$\int d\Gamma d\Gamma' P_{\text{eq}}(\Gamma) u_i' w(\Gamma \rightarrow \Gamma') = - \int d\Gamma^* P_{\text{eq}}(\Gamma^*) u_i^* \quad (124)$$

$$= \langle u_i \rangle$$

According to the transition probability in eq. (110), using eq. (78), we can write

$$\int d\Gamma P_{\text{eq}}(\Gamma) \left[ \frac{1}{2} \sum_{j \neq i} (\mathbf{v}_i - \mathbf{v}_j) \cdot \mathbf{e}_{ij} \gamma_{ij} \mathbf{e}_{ij} \cdot (\mathbf{v}_i - \mathbf{v}_j) \delta t \quad (125)$$

$$- \frac{1}{2m_i} \sum_{j \neq i} \sum_{l \neq i} \langle \delta \mathbf{p}_{ij}^R \cdot \delta \mathbf{p}_{il}^R \rangle_{\xi} + \dot{q}_i \delta t + \sum_{j \neq i} \langle \delta u_{ij}^R \rangle_{\xi} \right] = 0$$

The contribution due the conservative force has not been included since it identically vanishes because positions and velocities are uncorrelated in equilibrium. The same occurs with the term  $1/2 \sum_{j \neq i} (\mathbf{v}_i - \mathbf{v}_j) \cdot \delta \mathbf{p}_{ij}^R$ , as causality indicates that the random momenta is not correlated with the actual value of the velocity. Moreover, the first and second term identically cancel, in view of the fluctuation-dissipation theorem derived in the previous subsection. Therefore, we are left with

$$\int d\Gamma P_{\text{eq}}(\Gamma) \left( \dot{q}_i \delta t + \sum_{j \neq i} \langle \delta u_{ij}^R \rangle_{\xi} \right) = 0$$

We can now introduce the explicit expression for the heat flow, and of course, a change in the integration variables from  $\Gamma$  to  $\tilde{\Gamma}$  is in order

$$\int d\tilde{\Gamma} P_{\text{eq}}(\tilde{\Gamma}) \left[ - \sum_{j \neq i} \kappa_{ij} \left( \frac{1}{\tau_j} - \frac{1}{\tau_i} \right) \delta t - \kappa_i \left( \frac{1}{T} - \frac{1}{\tau_i} \right) \delta t + \sum_{j \neq i} \langle \delta u_{ij}^R \rangle_{\xi} \right] = 0$$

As  $\langle 1/\tau_i \rangle = 1/T$ , it follows that  $\langle \delta u_{ij}^R \rangle_{\xi} = 0$ . Therefore, this particular form of the heat flow introduces no spurious drift in the equation of motion that should be compensated.

The evaluation of the second moment of the energy distribution is more involved due to the number of terms that appear in its evaluation. Effectively proceeding as in eq. (117), we can write

$$\int d\Gamma d\Gamma' P_{\text{eq}}(\Gamma) u_i' u_j' w(\Gamma \rightarrow \Gamma') = \int d\Gamma^* P_{\text{eq}}(\Gamma^*) u_i^* u_j^* \quad (126)$$

$$= \langle u_i u_j \rangle$$

Then, using the dynamics equation (110), one can write

$$\int d\Gamma P_{\text{eq}}(\Gamma) \left( \left\{ u_i \left[ \frac{1}{2} \sum_{k \neq j} \left( \frac{\mathbf{p}_j - \mathbf{p}_k}{m} - \frac{\mathbf{p}_k}{m} \right) \cdot \boldsymbol{\gamma}_{jk} \cdot \left( \frac{\mathbf{p}_j - \mathbf{p}_k}{m} - \frac{\mathbf{p}_k}{m} \right) \delta t \quad (127)$$

$$- \frac{1}{2m} \sum_{k \neq j} \sum_{l \neq j} \langle \delta \mathbf{p}_{jk}^R \cdot \delta \mathbf{p}_{jl}^R \rangle_{\xi} \right\} + (i \leftrightarrow j)$$

$$+ (u_i q_j + u_j q_i) \delta t + \langle \delta u_i^R \delta u_j^R \rangle_{\xi}$$

$$+ \frac{1}{4} \sum_{k \neq i} \sum_{l \neq j} \left( \frac{\mathbf{p}_i - \mathbf{p}_k}{m} - \frac{\mathbf{p}_k}{m} \right) \cdot \langle \delta \mathbf{p}_{ik}^R \delta \mathbf{p}_{jl}^R \rangle_{\xi} \cdot \left( \frac{\mathbf{p}_j - \mathbf{p}_l}{m} - \frac{\mathbf{p}_l}{m} \right) \delta t \right) = 0$$

We can perform the integration with respect to momenta and use the fluctuation-dissipation theorem for the random momenta [eq. (122)]. Then, the terms involving momenta exactly cancel as

$$\int d\Gamma P_{\text{eq}}(\Gamma) \left\{ \left( u_i \frac{k_B T}{m} \sum_{l \neq j} \gamma_{jl} + u_j \frac{k_B T}{m} \sum_{k \neq i} \gamma_{ik} \right) \quad (128)$$

$$- \frac{1}{2m} \left[ u_i \sum_{l \neq j} k_B (\theta_j + \theta_l) \gamma_{jl} + u_j \sum_{k \neq i} k_B (\theta_i + \theta_k) \gamma_{ik} \right]$$

$$+ \frac{k_B T}{2m} \left[ \sum_{k \neq i} k_B (\theta_i + \theta_k) \gamma_{ik} \delta_{ij} + k_B (\theta_i + \theta_j) \gamma_{ij} \right] \right\} = 0$$

The third term is precisely the correlation between  $u$  and  $\theta$  appearing in the second term, given by

$$\int ds_j u_i \theta_j e^{s_j/k_B - u_j/(k_B T)}$$

$$= T u_i - k_B T \int ds_j u_i \frac{\partial}{\partial s_j} e^{s_j/k_B - u_j/(k_B T)} \quad (129)$$

$$= T u_i + k_B T^2 \delta_{ij}$$

We are then left with

$$\int d\Gamma P_{\text{eq}}(\Gamma) \left[ (u_i q_j + u_j q_i) \delta t + \langle \delta u_i^R \delta u_j^R \rangle_{\xi} \right] = 0 \quad (130)$$

and

$$\int d\Gamma P_{\text{eq}}(\Gamma) \left( -u_j \sum_k \kappa_{ik} \frac{1}{\tau_k} \delta t - u_i \sum_l \kappa_{jl} \frac{1}{\tau_l} \delta t \quad (131)$$

$$+ \langle \delta u_i^R \delta u_j^R \rangle_{\xi} \right) = 0$$

where we have introduced  $\kappa_{ii} \equiv -\sum_{j \neq i} \kappa_{ij}$ , for compactness. According to eq. (80), the random energy correlation has the form

$$\langle \delta u_i^R \delta u_j^R \rangle_{\xi} = \sum_{k \neq i} \sum_{l \neq j} \alpha_{ik} \alpha_{jl} \langle \xi_{ik} \xi_{jl} \rangle \delta t \quad (132)$$

$$= \left[ \sum_{k \neq i} \alpha_{ik}^2 \delta_{ij} - \alpha_{ij}^2 (1 - \delta_{ij}) \right] \delta t$$

On the other hand, let us assume for the moment that  $j \neq i$ , and focus our attention primarily on the integration with respect to the internal energy. Noticing that as the algorithm proposes the exchange of heat at constant volume ( $n_i = \text{const}$ ), then  $\sum_j \kappa_{jl} / \tau_l = 0$  and  $\sum_i u_i = U = \text{const}$  in the process. Then, imposing this last constraint in the integrand, changing the independent variables, we can readily integrate with respect to  $u_j$ , to obtain

$$\int du_1 \dots du_N e^{Z/k_B} \left( u_i \sum_k \kappa_{jk} \frac{1}{\tau_k} \right) \quad (133)$$

$$= k_B \int du_1 \dots du_N \left( u_i \sum_{l \neq j} \kappa_{jl} \frac{\partial}{\partial u_l} e^{\tilde{Z}/k_B} \right)$$

where  $Z \equiv \sum_i z_i$ , and  $\tilde{Z}$  represents  $Z$  with  $u_j = U - \sum_{l \neq j} u_l$ . Then, using partial integration with respect to  $u_l$ , we obtain

$$- \int du_1 \dots du_N e^{Z/k_B} \left( u_i \sum_k \kappa_{jk} \frac{1}{\tau_k} \right)$$

$$= k_B \int du_1 \dots du_N \left( \sum_{l \neq j} \kappa_{jl} \delta_{il} \right) e^{\tilde{Z}/k_B} \quad (134)$$

$$= k_B \kappa_{ij}$$

The term  $i = j$  can be readily obtained by realising that  $u_j = U - \sum_{l \neq j} u_l$ , which is introduced instead of  $u_i$  in eq. (133). The integration can be carried out in the same way to give

$$- \int du_1 \dots du_N e^{Z/k_B} \left( u_i \sum_k \kappa_{jk} \frac{1}{\tau_k} \right) \quad (135)$$

$$= -k_B \sum_{l \neq j} \kappa_{jl}$$

Comparing eq. (132) with eqs. (134) and (135), we arrive to the fluctuation-dissipation theorem, namely

$$\alpha_{ij} = \sqrt{2k_B \kappa_{ij}} \quad (136)$$

which agrees with eq. (81).

## Notes and references

- 1 S. Kopilevich, A. Gil, M. Garcia-Rates, J. Bonet Avalos, C. Bo, A. Mueller and I. A. Weinstock, *J. Am. Chem. Soc.*, 2012, **134**, 13082–13088.
- 2 G. Galli and D. Donadio, *Nat. Nanotechnol.*, 2010, **5**, 701–702.
- 3 G. Casati, *Nat. Nanotechnol.*, 2007, **2**, 23–24.
- 4 G. Stoltz, *Europhys. Lett.*, 2006, **76**, 849–855.
- 5 J. K. Brennan, M. Lísal, J. D. Moore, S. Izvekov, I. V. Schweigert and J. P. Larentzos, *J. Phys. Chem. Lett.*, 2014, **5**, 2144–2149.
- 6 O. Y. Fajardo, F. Bresme, A. A. Kornyshev and M. Urbakh, *Sci. Rep.*, 2015, **5**, 7698.
- 7 C. Luo and J.-U. Sommer, *Phys. Rev. Lett.*, 2009, **102**, 147801.
- 8 C. Liu and Z. Li, *Phys. Rev. Lett.*, 2010, **105**, 174501.
- 9 H. Patel, S. Garde and P. Keblinski, *Nano Lett.*, 2005, **5**, 2225–2231.
- 10 F. Bresme, A. Lervik, D. Bedeaux and S. Kjelstrup, *Phys. Rev. Lett.*, 2008, **101**, 020602.
- 11 J. D. Olarte-Plata and F. Bresme, *Phys. Chem. Chem. Phys.*, 2019, **21**, 1131–1140.
- 12 M. Hu, J. Goicoechea, B. Michel and D. Poulidakos, *Appl. Phys. Lett.*, 2009, **95**, 151903.
- 13 H. Acharya, N. J. Mozdzierz, P. Keblinski and S. Garde, *Ind. Eng. Chem. Res.*, 2012, **51**, 1767–1773.
- 14 A. Lervik, F. Bresme and S. Kjelstrup, *Soft Matter*, 2009, **5**, 2407–2414.
- 15 J. Muscatello, E. Chacón, P. Tarazona and F. Bresme, *Phys. Rev. Lett.*, 2017, **119**, 045901.
- 16 K. M. Lebold and W. G. Noid, *J. Chem. Phys.*, 2019, **150**, 014104.
- 17 J. P. Larentzos, J. M. Mansell, M. Lísal and J. K. Brennan, *Mol. Phys.*, 2018, **116**, 3271–3282.
- 18 Z. Li, Y.-H. Tang, H. Lei, B. Caswell and G. E. Karniadakis, *J. Comput. Phys.*, 2014, **265**, 113–127.
- 19 R. D. Groot and P. B. Warren, *J. Chem. Phys.*, 1997, **107**, 4423–4435.
- 20 J. B. Avalos and A. D. Mackie, *Europhys. Lett.*, 1997, **40**, 141–146.
- 21 P. Espanol, *Europhys. Lett.*, 1997, **40**, 631–636.
- 22 A. D. Mackie, J. B. Avalos and V. Navas, *Phys. Chem. Chem. Phys.*, 1999, **1**, 2039–2049.
- 23 E. Moeendarbary, T. Y. Ng and M. Zangeneh, *Int. J. Appl. Mech.*, 2009, **1**, 737–763.
- 24 R. Qiao and P. He, *Mol. Simul.*, 2007, **33**, 677–683.
- 25 T. Yamada, A. Kumar, Y. Asako, O. J. Gregory and M. Faghri, *Numer. Heat Transfer, Part A*, 2011, **60**, 651–665.
- 26 M. Lísal, J. K. Brennan and J. B. Avalos, *J. Chem. Phys.*, 2011, **135**, 204105.
- 27 P. Espanol and P. B. Warren, *J. Chem. Phys.*, 2017, **146**, 150901.
- 28 J. B. Maillat, E. Bourasseau, N. Desbiens, G. Vallverdu and G. Stoltz, *Europhys. Lett.*, 2011, **96**, 68007.
- 29 M. P. Kroonblawd, T. D. Sewell and J.-B. Maillat, *J. Chem. Phys.*, 2016, **144**, 064501.
- 30 G. C. Ganzenmüller, S. Hiermaier and M. O. Steinhauser, *Soft Matter*, 2011, **7**, 4307–4317.
- 31 J. D. Moore, B. C. Barnes, S. Izvekov, M. Lísal, M. S. Sellers, D. E. Taylor and J. K. Brennan, *J. Chem. Phys.*, 2016, **144**, 104501.
- 32 Z. Li, Y.-H. Tang, X. Li and G. E. Karniadakis, *Chem. Comm.*, 2015, **51**, 11038–11040.
- 33 E. O. Johansson, T. Yamada, B. Sundén and J. Yuan, *Int. J. Therm. Sci.*, 2016, **101**, 207–216.
- 34 I. Pagonabarraga and D. Frenkel, *J. Chem. Phys.*, 2001, **115**, 5015.
- 35 P. B. Warren, *Phys. Rev. Lett.*, 2001, **87**, 225702.
- 36 S. Y. Trofimov, E. L. F. Nies and M. A. J. Michels, *J. Chem. Phys.*, 2002, **117**, 9383–9394.
- 37 L. B. Lucy, *Astron. J.*, 1977, **82**, 1013–1024.

- 38 R. A. Gingold and J. J. Monaghan, *Mon. Not. R. Astron. Soc.*, 1977, **181**, 375–389.
- 39 P. Espanol and M. Revenga, *Phys. Rev. E*, 2003, **67**, 026705.
- 40 G. Faure, J.-B. Maillet, J. Roussel and G. Stoltz, *Phys. Rev. E*, 2016, **94**, 043305.
- 41 A. Vazquez-Quesada, M. Ellero and P. Espanol, *J. Chem. Phys.*, 2009, **130**, 034901.
- 42 S. Masgallie and P. A. Raviart, *Numer. Math.*, 1987, **51**, 323–352.
- 43 R. Di Lisio, E. Grenier and M. Pulvirenti, *Comput. Math. Appls.*, 1998, **35**, 95–102.
- 44 N. J. Quinlan, M. Basa and M. Lastiwka, *Int. J. Numer. Methods Eng.*, 2006, **66**, 2064–2085.
- 45 P. Langevin, *C. R. Hebd. Seances Acad. Sci.*, 1908, **146**, 530–533.
- 46 R. Zwanzig, *Nonequilibrium statistical mechanics*, Oxford University Press, 198 Madison Avenue, New York, New York 10016, 2001.
- 47 D. Keller, D. Swigon and C. Bustamante, *Biophys. J.*, 2003, **84**, 733–738.
- 48 C. Bustamante, J. Liphardt and F. Ritort, *Phys. Today*, 2005, **58**, 43–48.
- 49 T. Shardlow, *SIAM J. Sci. Comput.*, 2003, **24**, 1267–1282.
- 50 E. G. Flekkoy and P. V. Coveney, *Phys. Rev. Lett.*, 1999, **83**, 1775–1778.
- 51 E. G. Flekkoy, P. V. Coveney and G. De Fabritiis, *Phys. Rev. E*, 2000, **62**, 2140–2157.
- 52 G. Faure, J.-B. Maillet and G. Stoltz, *J. Chem. Phys.*, 2014, **117**, 114105.
- 53 *Here we have borrowed the term bare from Quantum Field Theory to describe, in a loose manner, a quantity whose magnitude is not affected by the fluctuations. In turn, dressed refers to a quantity whose magnitude is affected by the fluctuations.*
- 54 H. B. Callen, *Thermodynamics and an introduction to thermostatistics*, John Wiley & Sons., 1985.
- 55 D. C. Johnston, *Advances in thermodynamics of the van der Waals fluid*, Morgan & Claypool Publishers, 2014.
- 56 S. R. de Groot and P. Mazur, *Non-equilibrium thermodynamics*, Dover Publications., New York, USA, 1984.
- 57 N. G. Kampen, *Stochastic processes in physics and chemistry*, North Holland, Amsterdam, 1992.
- 58 M. P. Allen and D. J. Tildesley, *Computer simulation of liquids*, Clarendon Press, Cambridge, UK, 1987.
- 59 J. Kolafa and I. Nezbeda, *Fl. Ph. Eql.*, 1994, **100**, 1–34.
- 60 I. Pagonabarraga and D. Frenkel, *Molec. Simul.*, 2000, **25**, 167–175.
- 61 S. J. Plimpton, *J. Comput. Phys.*, 1995, **117**, 1–19.
- 62 D. Frenkel and B. Smit, *Understanding molecular simulation*, Academic Press, 2002.
- 63 P. B. Warren, *Phys. Rev. E*, 2013, **87**, 045303.
- 64 G. Stoltz, *J. Comput. Phys.*, 2017, **340**, 451–469.
- 65 A. Panagiotopoulos, N. Quirke, M. Stapleton and D. J. Tildesley, *Mol. Phys.*, 1988, **63**, 527–545.
- 66 P. Vanya, P. Crout, J. Sharman and J. A. Elliott, *Phys. Rev. E*, 2018, **63**, 033310.
- 67 J. J. Monaghan, *Rep. Prog. Phys.*, 2005, **68**, 1703–1759.
- 68 J. von Neumann, in *Von Neumann collected works*, ed. A. Taub, Pergamon, 1963, ch. Proposal and analysis of a new numerical method for the treatment of hydrodynamical shock problems (1944).
- 69 S. Izvekov, P. W. Chung and B. M. Rice, *J. Chem. Phys.*, 2010, **133**, 064109.
- 70 S. Izvekov, P. W. Chung and B. M. Rice, *J. Chem. Phys.*, 2011, **135**, 044112.
- 71 S. Izvekov and B. M. Rice, *J. Chem. Phys.*, 2014, **140**, 104104.
- 72 S. Izvekov and B. M. Rice, *Phys. Chem. Chem. Phys.*, 2015, **17**, 10795–10804.
- 73 Z. Li, H. S. Lee, E. Darve and G. E. Karniadakis, *J. Chem. Phys.*, 2017, **146**, 014104.
- 74 C. Hijon, P. Espanol, E. Vanden-Eijnden and R. Delgado-Buscalioni, *Faraday Discuss.*, 2010, **144**, 301–322.
- 75 Z. Li, X. Bian, X. Li and G. E. Karniadakis, *J. Chem. Phys.*, 2015, **143**, 243128.
- 76 A. Dequidt and J. G. S. Canchaya, *J. Chem. Phys.*, 2015, **143**, 084122.
- 77 J. G. S. Canchaya, A. Dequidt, F. Goujon and P. Malfreyt, *J. Chem. Phys.*, 2016, **145**, 054107.
- 78 D. Straub, I. Papaioannou and W. Betz, *J. Comput. Phys.*, 2016, **314**, 538–556.
- 79 V. Harmandaris, E. Kalligiannaki, M. Katsoulakis and P. Plecháč, *J. Comput. Phys.*, 2016, **314**, 355–383.
- 80 P. Vanya, J. Sharman and J. A. Elliot, *J. Chem. Phys.*, 2019, **150**, 064101.
- 81 L. Onsager and S. Machlup, *Phys. Rev.*, 1953, **91**, 1505–1512.

Energy-conserving dissipative particle dynamics method appropriate for particle interaction force fields that are both density- and temperature-dependent.

